White Rose Research Online

eprints@whiterose.ac.uk
https://eprints.whiterose.ac.uk
Universities of Leeds, Sheffield and York

Deposited via The University of Leeds.

White Rose Research Online URL for this paper:
https://eprints.whiterose.ac.uk/id/eprint/193353/

Version: Accepted Version

Article:
Karageorghis, A, Lesnic, D and Marin, L (2023) An efficient moving pseudo-boundary MFS for void detection. Engineering Analysis with Boundary Elements, 147. pp. 90-111. ISSN: 0955-7997

https://doi.org/10.1016/j.enganabound.2022.11.022

© 2022, Elsevier. This manuscript version is made available under the CC-BY-NC-ND 4.0 license http://creativecommons.org/licenses/by-nc-nd/4.0/.

Reuse
Items deposited in White Rose Research Online are protected by copyright, with all rights reserved unless indicated otherwise. They may be downloaded and/or printed for private study, or other acts as permitted by national copyright laws. The publisher or other rights holders may allow further reproduction and re-use of the full text version. This is indicated by the licence information on the White Rose Research Online record for the item.

Takedown
If you consider content in White Rose Research Online to be in breach of UK law, please notify us by emailing eprints@whiterose.ac.uk including the URL of the record and the reason for the withdrawal request.

UNIVERSITY OF LEEDS
University of Sheffield
UNIVERSITY of York

AN EFFICIENT MOVING PSEUDO–BOUNDARY MFS FOR VOID DETECTION

ANDREAS KARAGEORGHIS, DANIEL LESNIC, AND LIVIU MARIN

Abstract. We consider the method of fundamental solutions (MFS) for the determination of the boundary of a void. In the proposed formulation the location of the pseudo–boundary is not fixed. The MFS discretization of the corresponding inverse geometric boundary value problem yields a system of nonlinear equations in which the coefficients in the MFS approximation, the discrete radii in the polar parametrization, the coordinates of the centre of the void and the expansion and dilation coefficients of the pseudo–boundaries are unknown. For the minimization of the resulting functional we employ the nonlinear least squares minimization routine `lsqnonlin` from the MATLAB® optimization toolbox . In contrast to previous studies, we exploit the option which enables the user to provide the analytical expression for the Jacobian of the system, and show that, although tedious, this leads to spectacular savings in computational time. The case of multiple voids is also addressed.

1. Introduction

When a mathematical model is governed by a partial differential equation (PDE) which possesses a fundamental solution available explicitly, the underlying solution can be represented in terms of a single–layer or a double–layer potential (or a combination of these). Although this formulation reduces the dimensionality of the problem by one, the boundary integrals involved become singular when they are collocated at a boundary point in order to impose the given boundary conditions. One way to deal with this is to de–singularise them by shifting the integral over the boundary to that over a fictitious pseudo-boundary embracing the solution domain in its interior [12], provided that the smoothness of the data and geometry are sufficient to allow an analytic continuation of the field to the pseudo–boundary, [25]. The resulting method is nowadays known as the method of fundamental solutions (MFS) which has become a versatile, easy to use and accurate meshless numerical method for solving a wide range of both direct and inverse problems [8, 18], and, in particular, inverse geometric problems [19]. These latter problems are difficult to solve because they are both nonlinear and ill–posed. Nonlinear optimization techniques including regularization are therefore necessary.

In a previous study [16], we considered similar inverse boundary value problems (BVPs) to the ones studied in the current work. We used the MATLAB® optimization toolbox routine `lsqnonlin` without exploiting the option which enables the user to provide the analytical expression for the

Date: November 14, 2022.

2000 *Mathematics Subject Classification.* Primary 65N35; Secondary 65N21, 65N38.

Key words and phrases. Void detection, inverse problem, method of fundamental solutions.

Jacobian of the system, which is calculated approximately internally. Note that the Jacobian in the context of the application of the MFS to nonlinear BVPs using `lsqnonlin` was provided in [10]. Problems similar to those considered in the current work were studied with the boundary function method in [23, 27].

2. Mathematical formulation

A physical problem to which the MFS is most naturally suited and its application advantageous consists of the geometrical identification of an unknown void Ω_1 compactly contained and concealed in a surrounding container Ω_2 from non-destructive measurements on the boundary $\partial\Omega_2$ of the container. The process of scanning is based on electrostatics or steady-state heat conduction for which the governing PDE is the Laplace equation

$$\Delta u = 0 \quad \text{in} \quad \Omega := \Omega_2 \backslash \Omega_1, \tag{2.1a}$$

for the electrical potential or steady-state temperature u. In the above the annular material $\Omega \subset \mathbb{R}^{\mathrm{n}}$, $\mathrm{n} = 2, 3$, is assumed homogeneous, but anisotropic, nonlinear, layered or functionally graded materials are also feasible in the context of the MFS [3, 21].
In the investigation of this paper, the unknown void Ω_1 is a rigid inclusion, on whose boundary the homogeneous Dirichlet boundary condition

$$u = 0 \quad \text{on} \quad \partial\Omega_1 \tag{2.1b}$$

applies, or a cavity, on whose boundary the homogeneous Neumann boundary condition

$$\partial_n u = 0 \quad \text{on} \quad \partial\Omega_1 \tag{2.1c}$$

applies, where $\boldsymbol{n}$ is the outward unit normal vector. Composite materials of different finite conductivity such that the void Ω_1 is an unknown inclusion can also be considered [15]. We can unify the boundary conditions (2.1b) and (2.1c) into a single boundary condition written as

$$\alpha u + (1-\alpha)\partial_n u = 0 \quad \text{on} \quad \partial\Omega_1\,, \quad \text{where} \quad \alpha \in \{0, 1\}. \tag{2.1d}$$

On the boundary $\partial\Omega_2$ of the container Ω_2, any type of boundary condition can be prescribed, e.g. Dirichlet

$$u = f \quad \text{on} \quad \partial\Omega_2, \tag{2.1e}$$

or Neumann

$$\partial_n u = g \quad \text{on} \quad \partial\Omega_2. \tag{2.1f}$$

When $\alpha = 0$, for (2.1a), (2.1d) and (2.1f) to be consistent, we require

$$\int_{\partial\Omega_2} g \, ds = 0. \tag{2.2}$$

We assume that the annular solution domain $\Omega = \Omega_2 \backslash \Omega_1$ is connected and that its boundary $\partial\Omega = \partial\Omega_1 \cup \partial\Omega_2$ is sufficiently smooth, e.g. of class $\mathcal{C}^2$. Then, if Ω_1 is known, the direct linear and well-posed problem given by equations (2.1a), (2.1d) and (2.1e) (or (2.1f) and (2.2)) has a unique weak solution $u \in H^1(\Omega)$ if $f \in H^{1/2}(\partial\Omega_2)$ (or if $g \in H^{-1/2}(\partial\Omega_2)$), and a unique classical solution

$u \in \mathcal{C}^2(\Omega) \cap \mathcal{C}(\bar{\Omega})$, if f (or g) is sufficiently smooth, see e.g. [26].

In contrast to the direct (forward) problem, where Ω_1 is known, the resulting inverse nonlinear and ill-posed problem consists of determining the pair (u, Ω_1) satisfying the Laplace equation (2.1a), given the Dirichlet data $f \not\equiv$ constant in (2.1e), the homogeneous boundary condition (2.1d) and the Neumann current flux measurement (2.1f). Although the solution is unique, see [1, 11, 24], it is unstable with respect to small errors in the input Cauchy data (2.1e) and (2.1f).

3. The method of fundamental solutions (MFS)

Consider, for simplicity, two-dimensions [16] but similar considerations can be applied to three-dimensions [17] as well. In the application of the MFS to the Laplace equation (2.1a), the solution is approximated by a linear combination of fundamental solutions [14]

$$u_N(\boldsymbol{c}, \boldsymbol{\xi}; \boldsymbol{x}) = \sum_{k=1}^{2N} c_k \, G(\boldsymbol{\xi}_k, \boldsymbol{x}), \quad \boldsymbol{x} \in \overline{\Omega}, \tag{3.1}$$

where G is the fundamental solution of the two–dimensional Laplace operator, given by

$$G(\boldsymbol{\xi}, \boldsymbol{x}) = -\frac{1}{2\pi} \ln |\boldsymbol{\xi} - \boldsymbol{x}|. \tag{3.2}$$

Note that throughout the paper we adopt the notation $\overline{1, \mathcal{N}} = 1, \ldots, \mathcal{N}$. In this formulation, a total of $2N$ sources $(\boldsymbol{\xi}_k)_{k=\overline{1,2N}}$ are placed outside the domain Ω, i.e. in $\Omega_1 \cup \left(\mathbb{R}^2 \backslash \bar{\Omega}_2\right)$. The first N of these sources, $(\boldsymbol{\xi}_k)_{k=\overline{1,N}}$, are placed in Ω_1, on a pseudo–boundary $\partial\Omega_1'$ similar to $\partial\Omega_1$. By *similar* we mean a dilation or a contraction of a given star–like boundary about its centre. The remaining N sources $(\boldsymbol{\xi}_k)_{k=\overline{N+1,2N}}$ are placed in $\mathbb{R}^2 \backslash \overline{\Omega}_2$, on a pseudo–boundary $\partial\Omega_2'$ similar to $\partial\Omega_2$. A typical distribution of sources is depicted in Figure 1. It should be stated that in the current approach the two pseudo–boundaries $\partial\Omega_1'$ and $\partial\Omega_2'$ are not fixed and their final locations will be determined as part of the solution (moving pseudo–boundaries). The idea of taking similar pseudo–boundaries to the physical boundaries yields, in general, more accurate MFS results [9, 20].
In the current study, we shall take, for simplicity, the exterior boundary $\partial\Omega_2$ to be a circle of radius R, hence the sources on $\partial\Omega_2'$ will be

$$\boldsymbol{\xi}_{N+k} = \eta_{\text{ext}} \, R \, (\cos \vartheta_k, \sin \vartheta_k), \quad \vartheta_k = \frac{2\pi(k-1)}{N}, \quad k = \overline{1, N}, \tag{3.3}$$

and the unknown dilation parameter η_{ext} will lie in the interval $(1, S)$ with $S > 1$ prescribed. We shall also assume that the unknown boundary $\partial\Omega_1$ is a smooth, star–like curve with respect to the centre coordinates (X, Y) which are also unknown. Hence, in polar coordinates the equation of $\partial\Omega_1$ is

$$x = X + r(\vartheta) \cos \vartheta, \qquad y = Y + r(\vartheta) \sin \vartheta, \qquad \vartheta \in [0, 2\pi), \tag{3.4}$$

where r is a smooth $2\pi-$periodic function. By denoting

$$r_k = r(\vartheta_k), \quad k = \overline{1, N}, \tag{3.5}$$

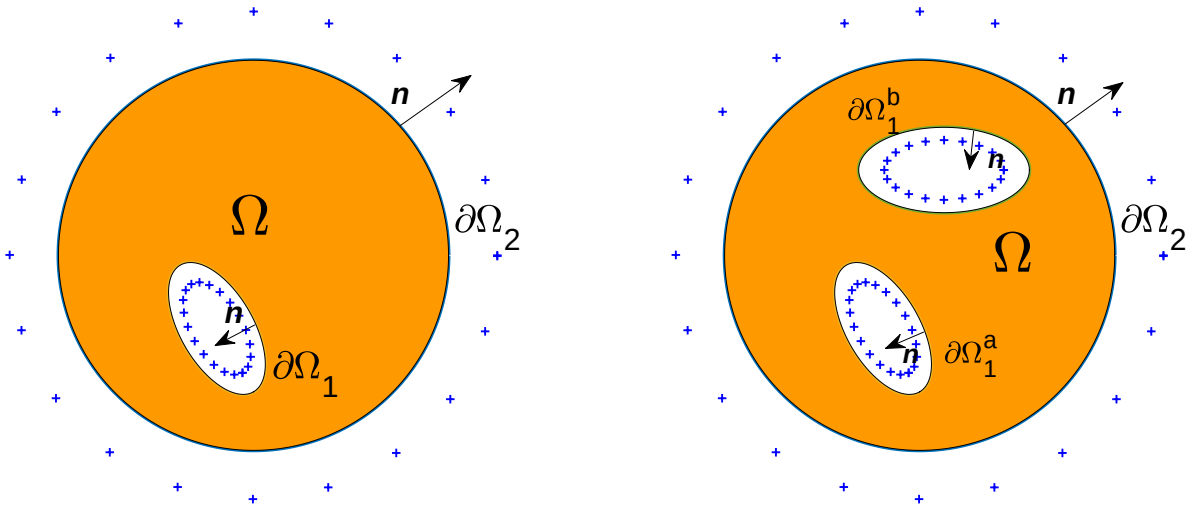

(a) One inclusion (b) Two inclusions

FIGURE 1. Geometry of problem with (a) One inclusion. (b) Two inclusions. The crosses (+) denote the sources.

the source points on $\partial\Omega_1'$ will be

$$\boldsymbol{\xi}_k = (X, Y) + \eta_{\text{int}}\, r_k\, (\cos\vartheta_k, \sin\vartheta_k)\,, \quad k = \overline{1, N}, \tag{3.6}$$

where the unknown contraction parameter η_{int} lies in the interval $(0, 1)$. In addition to the sources we shall also define $M + N$ boundary collocation points. The first N of these, $(\boldsymbol{x}_k)_{k=\overline{1,N}}$ will be placed on $\partial\Omega_1$, as follows:

$$\boldsymbol{x}_k = (X, Y) + r_k\, (\cos\vartheta_k, \sin\vartheta_k)\,, \quad k = \overline{1, N}. \tag{3.7}$$

The remaining M points $(\boldsymbol{x}_{N+\ell})_{\ell=\overline{1,M}}$ will be placed on $\partial\Omega_2$, i.e.

$$\boldsymbol{x}_{N+\ell} = R\,(\cos\tilde{\vartheta}_\ell, \sin\tilde{\vartheta}_\ell), \quad \ell = \overline{1, M}, \quad \tilde{\vartheta}_\ell = \frac{2\pi(\ell - 1)}{M}, \quad \ell = \overline{1, M}. \tag{3.8}$$

4. Implementation details

In the MFS formulation for the solution of inverse problem given by equations (2.1a), (2.1e), (2.1d) and (2.1f), described in Section 3, we have the following unknowns:

- The coefficients $\boldsymbol{c} = (c_k)_{k=\overline{1,2N}}$ in (3.1),
- the radii $\boldsymbol{r} = (r_k)_{k=\overline{1,N}}$ in (3.5),
- the contraction and dilation coefficients $\boldsymbol{\eta} = (\eta_{\text{int}}, \eta_{\text{ext}})$ in (3.6) and (3.3), and
- the centre coordinates $\boldsymbol{C} = (X, Y)$.

The unknowns listed above are determined from the imposition of the boundary conditions (2.1e), (2.1d) and (2.1f) in a least-squares sense which leads to minimizing the functional

$$S(\boldsymbol{c},\boldsymbol{r},\boldsymbol{\eta},\boldsymbol{C}) := \sum_{j=N+1}^{N+M} \left[u_N(\boldsymbol{c},\boldsymbol{\xi};\boldsymbol{x}_j) - f(\boldsymbol{x}_j)\right]^2 + \sum_{j=N+1}^{N+M} \left[\partial_n u_N(\boldsymbol{c},\boldsymbol{\xi};\boldsymbol{x}_j) - g^{\varepsilon}(\boldsymbol{x}_j)\right]^2$$
$$+ \sum_{j=1}^{N} \left[\alpha u_N(\boldsymbol{c},\boldsymbol{\xi};\boldsymbol{x}_j) + (1-\alpha)\partial_n u_N(\boldsymbol{c},\boldsymbol{\xi};\boldsymbol{x}_j)\right]^2 + \lambda_1 |\boldsymbol{c}|^2 + \lambda_2 \sum_{\ell=2}^{N} \left(r_\ell - r_{\ell-1}\right)^2, \tag{4.1}$$

where λ_1 and $\lambda_2 \geq 0$ are regularization parameters that need to be prescribed and

$$g^{\varepsilon}(\boldsymbol{x}_j) = (1+\rho_j\, p)\, g(\boldsymbol{x}_j)\,, \quad j = \overline{N+1, N+M}, \tag{4.2}$$

where p represents the percentage of noise added to the Neumann boundary data on $\partial\Omega_2$ and ρ_j is a pseudo-random noisy variable drawn from a uniform distribution in $[-1,1]$ using the MATLAB® command `-1+2*rand(1,M)`. The outward normal vector $\boldsymbol{n}$ to the boundary, needed in the implementation of the method is defined in the Appendix. The regularization terms $\lambda_1|\boldsymbol{c}|^2$ and $\lambda_2 \sum_{\ell=2}^{N} (r_\ell - r_{\ell-1})^2$ have been added to the functional (4.1) to stabilize the MFS solution u_N and the $\mathcal{C}^1-$smooth boundary $\partial\Omega_1$. The summation in the last term of (4.1) has been taken from $\ell = 2$ to N in order to compare with the numerical results of [16], which considered the same expression. The summation can also be taken from $\ell = 2$ to $N+1$, with the convention that $r_{N+1} = r_1$, as considered in [4]. Finally, note that in (4.1) we have $3N+4$ unknowns and $N+2M$ boundary collocations equations so we need to take $M \geq N+2$.

4.1. **Non-linear minimization software.** In the current study, the least-squares minimization of functional (4.1) is achieved via the MATLAB® [22] optimization toolbox routine `lsqnonlin`. This, minimizes the general functional (cf. (4.1))

$$S(\mathbf{x}) := \sum_{j=1}^{\mathcal{J}} F_j^2, \tag{4.3}$$

with respect to the $\mathcal{M}$ unknowns $\mathbf{x} = [\mathrm{x}_1, \mathrm{x}_2, \ldots, \mathrm{x}_{\mathcal{M}}]^{\mathrm{T}}$.
The routine `lsqnonlin` by default uses the trust–region–reflective algorithm based on the interior-reflective Newton method [6,7] for minimizing the non-linear least-squares functional (4.3) starting from an initial guess $\mathbf{x}_0$. In the call to `lsqnonlin`, one is required to provide the functions F_j, $j = \overline{1,\mathcal{J}}$, in the functional (4.3). The user is also offered, via the optimization options, the choice of providing the Jacobian of the system analytically or not. In the latter case, the Jacobian is calculated internally. Otherwise, the exact Jacobian J is

$$J_{j,m} = \frac{\partial F_j}{\partial \mathrm{x}_m}, \quad j = \overline{1,\mathcal{J}},\ m = \overline{1,\mathcal{M}}.$$

When the Jacobian is not provided, the optimization options are called with
`options=optimoptions(@lsqnonlin,'Display','iter','MaxFunEvals',mf, ...`

`'MaxIter',mm,'TolFun',1.E-15,'TolX',1.E-15,'SpecifyObjectiveGradient',false)`
and the function call is
`[x,resnorm,residual,exitflag,output] = lsqnonlin(@f1,x0,options)`,
where the `function f=f1(x)` provides the functions F_j, $j=\overline{1,\mathcal{J}}$.

When the exact Jacobian is provided, the optimization options are changed to
`options=optimoptions(@lsqnonlin,'Display','iter','MaxFunEvals',mf, ...`
`'MaxIter',mm,'TolFun',1.E-15,'TolX',1.E-15,'SpecifyObjectiveGradient',true)`,
while the function call becomes `function [f,J]=f1(x)`, which provides both the functions F_j, $j=\overline{1,\mathcal{J}}$, (`f`), and the exact Jacobian $J_{j,m}$, $j=\overline{1,\mathcal{J}}$, $m=\overline{1,\mathcal{M}}$, (`J`).

The routine `lsqnonlin` terminates when

- the change in the solution vector $\mathbf{x}$ is less than the optimization options specified tolerance `TolX`, or
- the change in the residual is less than the optimization options specified tolerance `TolFun`, or
- the number of iterations `MaxIter` or the number of function evaluations `MaxFunEvals` (both specified in the optimization options) is exceeded.

Moreover, in `lsqnonlin` one has the option of imposing lower and upper bounds on the elements of the vector of unknowns $\mathbf{x}=[\boldsymbol{c},\boldsymbol{r},\boldsymbol{\eta},\boldsymbol{C}]^{\mathrm{T}}$ through the user–specified vectors `lb` and `up`. In our applications, we imposed the constraints $0<r_n<R,\quad n=\overline{1,N}$, $0<\eta_{\text{int}}<1$, $1<\eta_{\text{ext}}<4$ and $-R<X<R, -R<Y<R$.

4.2. **Derivation of Jacobian.** Some of the formulæ given below require the normal $\boldsymbol{n}_j=(n_{x_j},n_{y_j})$, $j=\overline{1,N}$, to the cavity boundary, which are provided in the Appendix. Moreover, the derivatives of the normals $\boldsymbol{n}_j$ with respect to the variables $r_m, m=\overline{1,N}$ are also provided in the Appendix. In the implementation we need to provide `lsqnonlin` with the following information (note that we use the notation $\gamma=-\dfrac{1}{2\pi}$):

$\alpha=1$.

$$F_j=\sum_{k=1}^{2N}c_k\,G(\boldsymbol{\xi}_k,\boldsymbol{x}_j)=\gamma\sum_{k=1}^{N}c_k\log\sqrt{\left(r_j\cos\vartheta_j-\eta_{\text{int}}r_k\cos\vartheta_k\right)^2+\left(r_j\sin\vartheta_j-\eta_{\text{int}}r_k\sin\vartheta_k\right)^2}$$

$$+\gamma\sum_{k=N+1}^{2N}c_k\log\sqrt{\left(X+r_j\cos\vartheta_j-\eta_{\text{ext}}R\cos\vartheta_{k-N}\right)^2+\left(Y+r_j\sin\vartheta_j-\eta_{\text{ext}}R\sin\vartheta_{k-N}\right)^2},\quad j=\overline{1,N},$$

$$J_{j,m}=G(\boldsymbol{\xi}_m,\boldsymbol{x}_j),\quad j=\overline{1,N},\ m=\overline{1,2N},$$

$$J_{j,2N+m} = \frac{\partial}{\partial r_m} \sum_{k=1}^{2N} c_k\, G(\boldsymbol{\xi}_k, \boldsymbol{x}_j)$$

$$= -\gamma\eta_{\text{int}} c_m \frac{(\boldsymbol{x}_j - \boldsymbol{\xi}_m)\cdot(\cos\vartheta_m, \sin\vartheta_m)}{|\boldsymbol{x}_j - \boldsymbol{\xi}_m|^2}, \quad m \neq j, \quad j = \overline{1,N},\ m = \overline{1,N},$$

$$J_{m,2N+m} = \frac{\partial}{\partial r_m} \sum_{k=1}^{2N} c_k\, G(\boldsymbol{\xi}_k, \boldsymbol{x}_j)$$

$$= -\gamma\eta_{\text{int}} c_m \frac{(\boldsymbol{x}_m - \boldsymbol{\xi}_m)\cdot(\cos\vartheta_m, \sin\vartheta_m)}{|\boldsymbol{x}_m - \boldsymbol{\xi}_m|^2} + \gamma \sum_{k=1}^{2N} c_k \frac{(\boldsymbol{x}_m - \boldsymbol{\xi}_k)\cdot(\cos\vartheta_m, \sin\vartheta_m)}{|\boldsymbol{x}_m - \boldsymbol{\xi}_k|^2}, \quad m = \overline{1,N},$$

$$J_{j,3N+1} = \sum_{k=1}^{2N} c_k \frac{\partial G(\boldsymbol{\xi}_k, \boldsymbol{x}_j)}{\partial \eta_{\text{int}}} = -\gamma \sum_{k=1}^{N} c_k r_k \frac{(\boldsymbol{x}_j - \boldsymbol{\xi}_k)\cdot(\cos\vartheta_k, \sin\vartheta_k)}{|\boldsymbol{x}_j - \boldsymbol{\xi}_k|^2}, \quad j = \overline{1,N},$$

$$J_{j,3N+2} = \sum_{k=1}^{2N} c_k \frac{\partial G(\boldsymbol{\xi}_k, \boldsymbol{x}_j)}{\partial \eta_{\text{ext}}} = -\gamma \sum_{k=N+1}^{2N} c_k R \frac{(\boldsymbol{x}_j - \boldsymbol{\xi}_k)\cdot(\cos\vartheta_{k-N}, \sin\vartheta_{k-N})}{|\boldsymbol{x}_j - \boldsymbol{\xi}_k|^2}, \quad j = \overline{1,N},$$

$$J_{j,3N+3} = \sum_{k=1}^{2N} c_k \frac{\partial G(\boldsymbol{\xi}_k, \boldsymbol{x}_j)}{\partial X} = \gamma \sum_{k=N+1}^{2N} c_k \frac{(\boldsymbol{x}_j - \boldsymbol{\xi}_k)_x}{|\boldsymbol{x}_j - \boldsymbol{\xi}_k|^2}, \quad j = \overline{1,N},$$

$$J_{j,3N+4} = \sum_{k=1}^{2N} c_k \frac{\partial G(\boldsymbol{\xi}_k, \boldsymbol{x}_j)}{\partial Y} = \gamma \sum_{k=N+1}^{2N} c_k \frac{(\boldsymbol{x}_j - \boldsymbol{\xi}_k)_y}{|\boldsymbol{x}_j - \boldsymbol{\xi}_k|^2}, \quad j = \overline{1,N}.$$

$\alpha = 0$.

$$F_j = \sum_{k=1}^{2N} c_k\, \partial_n G(\boldsymbol{\xi}_k, \boldsymbol{x}_j) = \gamma \sum_{k=1}^{2N} c_k \frac{(\boldsymbol{x}_j - \boldsymbol{\xi}_k)\cdot \boldsymbol{n}_j}{|\boldsymbol{x}_j - \boldsymbol{\xi}_k|^2}$$

$$= \gamma \sum_{k=1}^{N} c_k \frac{(r_j\cos\vartheta_j - \eta_{\text{int}} r_k \cos\vartheta_k)\, n_{x_j} + (r_j \sin\vartheta_j - \eta_{\text{int}} r_k \sin\vartheta_k)\, n_{y_j}}{(r_j\cos\vartheta_j - \eta_{\text{int}} r_k \cos\vartheta_k)^2 + (r_j \sin\vartheta_j - \eta_{\text{int}} r_k \sin\vartheta_k)^2}$$

$$+\gamma \sum_{k=N+1}^{2N} c_k \frac{(X + r_j\cos\vartheta_j - \eta_{\text{ext}} R\cos\vartheta_{k-N})\, n_{x_j} + (Y + r_j \sin\vartheta_j - \eta_{\text{ext}} R\sin\vartheta_{k-N})\, n_{y_j}}{(X + r_j\cos\vartheta_j - \eta_{\text{ext}} R\cos\vartheta_{k-N})^2 + (Y + r_j \sin\vartheta_j - \eta_{\text{ext}} R\sin\vartheta_{k-N})^2}, \ j = \overline{1,N},$$

. . . . . .

$$J_{j,m} = \partial_n G(\boldsymbol{\xi}_m, \boldsymbol{x}_j) = \gamma \frac{(\boldsymbol{x}_j - \boldsymbol{\xi}_m)\cdot \boldsymbol{n}_j}{|\boldsymbol{x}_j - \boldsymbol{\xi}_m|^2}, \quad j = \overline{1,N},\ m = \overline{1,2N},$$

$$J_{j,2N+m} = \frac{\partial}{\partial r_m} \sum_{k=1}^{2N} c_k\, \partial_n G(\boldsymbol{\xi}_k, \boldsymbol{x}_j)$$

$$= \gamma\eta_{\text{int}} c_m \left[-\frac{(\cos\vartheta_m, \sin\vartheta_m)\cdot \boldsymbol{n}_j}{|\boldsymbol{x}_j - \boldsymbol{\xi}_m|^2} + 2\frac{(\boldsymbol{x}_j - \boldsymbol{\xi}_m)\cdot \boldsymbol{n}_j}{|\boldsymbol{x}_j - \boldsymbol{\xi}_m|^4} \left((\boldsymbol{x}_j - \boldsymbol{\xi}_m)\cdot(\cos\vartheta_m, \sin\vartheta_m)\right) \right]$$

$$+\gamma\sum_{k=1}^{2N} c_k \frac{1}{|\boldsymbol{x}_j-\boldsymbol{\xi}_k|^2}\left((\boldsymbol{x}_j-\boldsymbol{\xi}_k)\cdot\frac{\partial \boldsymbol{n}_j}{\partial r_m}\right)$$

$$+\gamma\delta_{mj}\sum_{k=1}^{2N} c_k\left[\frac{(\cos\vartheta_j,\sin\vartheta_j)\cdot\boldsymbol{n}_j}{|\boldsymbol{x}_j-\boldsymbol{\xi}_k|^2}-2\frac{(\boldsymbol{x}_j-\boldsymbol{\xi}_k)\cdot\boldsymbol{n}_j}{|\boldsymbol{x}_j-\boldsymbol{\xi}_k|^4}\left((\boldsymbol{x}_j-\boldsymbol{\xi}_k)\cdot(\cos\vartheta_j,\sin\vartheta_j)\right)\right],$$

$$j=\overline{1,N},\ m=\overline{1,N},$$

$$J_{j,3N+1}=\frac{\partial}{\partial\eta_{\text{int}}}\sum_{k=1}^{N} c_k\,\partial_n G(\boldsymbol{\xi}_k,\boldsymbol{x}_j)$$

$$=\gamma\sum_{k=1}^{N} c_k r_k\left[-\frac{(\cos\vartheta_k,\sin\vartheta_k)\cdot\boldsymbol{n}_j}{|\boldsymbol{x}_j-\boldsymbol{\xi}_k|^2}+2\frac{(\boldsymbol{x}_j-\boldsymbol{\xi}_k)\cdot\boldsymbol{n}_j}{|\boldsymbol{x}_j-\boldsymbol{\xi}_k|^4}\left((\boldsymbol{x}_j-\boldsymbol{\xi}_k)\cdot(\cos\vartheta_k,\sin\vartheta_k)\right)\right],\quad j=\overline{1,N},$$

$$J_{j,3N+2}=\frac{\partial}{\partial\eta_{\text{ext}}}\sum_{k=N+1}^{2N} c_k\,\partial_n G(\boldsymbol{\xi}_k,\boldsymbol{x}_j)$$

$$=\gamma R\sum_{k=N+1}^{2N} c_k\left[-\frac{(\cos\vartheta_{k-N},\sin\vartheta_{k-N})\cdot\boldsymbol{n}_j}{|\boldsymbol{x}_j-\boldsymbol{\xi}_k|^2}+2\frac{(\boldsymbol{x}_j-\boldsymbol{\xi}_k)\cdot\boldsymbol{n}_j}{|\boldsymbol{x}_j-\boldsymbol{\xi}_k|^4}\left((\boldsymbol{x}_j-\boldsymbol{\xi}_k)\cdot(\cos\vartheta_{k-N},\sin\vartheta_{k-N})\right)\right],$$

$$j=\overline{1,N},$$

$$J_{j,3N+3}=\frac{\partial}{\partial X}\sum_{k=N+1}^{2N} c_k\,\partial_n G(\boldsymbol{\xi}_k,\boldsymbol{x}_j)$$

$$=\gamma\sum_{k=N+1}^{2N} c_k\left[\frac{n_{x_j}}{|\boldsymbol{x}_j-\boldsymbol{\xi}_k|^2}-2\frac{(\boldsymbol{x}_j-\boldsymbol{\xi}_k)\cdot\boldsymbol{n}_j}{|\boldsymbol{x}_j-\boldsymbol{\xi}_k|^4}\left(\boldsymbol{x}_j-\boldsymbol{\xi}_k\right)_x\right],\quad j=\overline{1,N},$$

$$J_{j,3N+4}=\frac{\partial}{\partial Y}\sum_{k=N+1}^{2N} c_k\,\partial_n G(\boldsymbol{\xi}_k,\boldsymbol{x}_j)$$

$$=\gamma\sum_{k=N+1}^{2N} c_k\left[\frac{n_{y_j}}{|\boldsymbol{x}_j-\boldsymbol{\xi}_k|^2}-2\frac{(\boldsymbol{x}_j-\boldsymbol{\xi}_k)\cdot\boldsymbol{n}_j}{|\boldsymbol{x}_j-\boldsymbol{\xi}_k|^4}\left(\boldsymbol{x}_j-\boldsymbol{\xi}_k\right)_y\right],\quad j=\overline{1,N},$$

$$F_j=\sum_{k=1}^{2N} c_k\,G(\boldsymbol{\xi}_k,\boldsymbol{x}_j)-f(\boldsymbol{x}_j)$$

$$=\gamma\sum_{k=1}^{N} c_k\log\sqrt{\left(R\cos\tilde{\vartheta}_{j-N}-X-\eta_{\text{int}}r_k\cos\vartheta_k\right)^2+\left(R\sin\tilde{\vartheta}_{j-N}-Y-\eta_{\text{int}}r_k\sin\vartheta_k\right)^2}$$

$$+\gamma\sum_{k=N+1}^{2N} c_k \log\sqrt{\left(R\cos\tilde{\vartheta}_{j-N}-\eta_{\rm ext}R\cos\vartheta_{k-N}\right)^2+\left(R\sin\tilde{\vartheta}_{j-N}-\eta_{\rm ext}R\sin\vartheta_{k-N}\right)^2}-f(\boldsymbol{x}_j),$$

$$j=\overline{N+1,N+M},$$

. . . . . .

$$J_{j,m}=G(\boldsymbol{\xi}_m,\boldsymbol{x}_j),\quad j=\overline{N+1,N+M},\ m=\overline{1,2N},$$

$$J_{j,2N+m}=\frac{\partial}{\partial r_m}\sum_{k=1}^{2N} c_k\,G(\boldsymbol{\xi}_k,\boldsymbol{x}_j)=-\gamma\eta_{\rm int}c_m\frac{(\boldsymbol{x}_j-\boldsymbol{\xi}_m)\cdot(\cos\vartheta_m,\sin\vartheta_m)}{|\boldsymbol{x}_j-\boldsymbol{\xi}_m|^2},$$

$$j=\overline{N+1,N+M},\ m=\overline{1,N},$$

$$J_{j,3N+1}=\sum_{k=1}^{2N} c_k\,\frac{\partial G(\boldsymbol{\xi}_k,\boldsymbol{x}_j)}{\partial\eta_{\rm int}}=-\gamma\sum_{k=1}^{N} c_k r_k\frac{(\boldsymbol{x}_j-\boldsymbol{\xi}_k)\cdot(\cos\vartheta_k,\sin\vartheta_k)}{|\boldsymbol{x}_j-\boldsymbol{\xi}_k|^2},\quad j=\overline{N+1,N+M},$$

$$J_{j,3N+2}=\sum_{k=1}^{2N} c_k\,\frac{\partial G(\boldsymbol{\xi}_k,\boldsymbol{x}_j)}{\partial\eta_{\rm ext}}=-\gamma\sum_{k=N+1}^{2N} c_k R\frac{(\boldsymbol{x}_j-\boldsymbol{\xi}_k)\cdot(\cos\vartheta_{k-N},\sin\vartheta_{k-N})}{|\boldsymbol{x}_j-\boldsymbol{\xi}_k|^2},\quad j=\overline{N+1,N+M},$$

$$J_{j,3N+3}=\sum_{k=1}^{2N} c_k\,\frac{\partial G(\boldsymbol{\xi}_k,\boldsymbol{x}_j)}{\partial X}=-\gamma\sum_{k=1}^{N} c_k\frac{(\boldsymbol{x}_j-\boldsymbol{\xi}_k)_x}{|\boldsymbol{x}_j-\boldsymbol{\xi}_k|^2},\quad j=\overline{N+1,N+M},$$

$$J_{j,3N+4}=\sum_{k=1}^{2N} c_k\,\frac{\partial G(\boldsymbol{\xi}_k,\boldsymbol{x}_j)}{\partial Y}=-\gamma\sum_{k=1}^{N} c_k\frac{(\boldsymbol{x}_j-\boldsymbol{\xi}_k)_y}{|\boldsymbol{x}_j-\boldsymbol{\xi}_k|^2},\quad j=\overline{N+1,N+M},$$

$$F_{M+j}=\sum_{k=1}^{2N} c_k\,\partial_n G(\boldsymbol{\xi}_k,\boldsymbol{x}_j)-g^{\varepsilon}(\boldsymbol{x}_j)=\gamma\sum_{k=1}^{2N} c_k\,\frac{(\boldsymbol{x}_j-\boldsymbol{\xi}_k)\cdot\boldsymbol{n}_j}{|\boldsymbol{x}_j-\boldsymbol{\xi}_k|^2}-g^{\varepsilon}(\boldsymbol{x}_j)$$

$$=\gamma\sum_{k=1}^{N} c_k\frac{\left(R\cos\tilde{\vartheta}_{j-N}-X-\eta_{\rm int}r_k\cos\vartheta_k\right)\cos\tilde{\vartheta}_{j-N}+\left(R\sin\tilde{\vartheta}_{j-N}-Y-\eta_{\rm int}r_k\sin\vartheta_k\right)\sin\tilde{\vartheta}_{j-N}}{\left(R\cos\tilde{\vartheta}_{j-N}-X-\eta_{\rm int}r_k\cos\vartheta_k\right)^2+\left(R\sin\tilde{\vartheta}_{j-N}-Y-\eta_{\rm int}r_k\sin\vartheta_k\right)^2}$$

$$+\gamma\sum_{k=N+1}^{2N} c_k\frac{\left(R\cos\tilde{\vartheta}_{j-N}-\eta_{\rm ext}R\cos\vartheta_{k-N}\right)\cos\tilde{\vartheta}_{j-N}+\left(R\sin\tilde{\vartheta}_{j-N}-\eta_{\rm ext}R\sin\vartheta_{k-N}\right)\sin\tilde{\vartheta}_{j-N}}{\left(R\cos\tilde{\vartheta}_{j-N}-\eta_{\rm ext}R\cos\vartheta_{k-N}\right)^2+\left(R\sin\tilde{\vartheta}_{j-N}-\eta_{\rm ext}R\sin\vartheta_{k-N}\right)^2}$$

$$-g^{\varepsilon}(\boldsymbol{x}_j),\quad j=\overline{N+1,N+M},$$

. . . . . .

$$J_{M+j,m}=\partial_n G(\boldsymbol{\xi}_m,\boldsymbol{x}_j)=\gamma\frac{(\boldsymbol{x}_j-\boldsymbol{\xi}_m)\cdot\boldsymbol{n}_j}{|\boldsymbol{x}_j-\boldsymbol{\xi}_m|^2},\quad j=\overline{N+1,N+M},\ m=\overline{1,2N},$$

$$J_{M+j,2N+m}=\frac{\partial}{\partial r_m}\sum_{k=1}^{2N} c_k\,\partial_n G(\boldsymbol{\xi}_k,\boldsymbol{x}_j)$$

$$= \gamma\eta_{\text{int}} c_m \left[-\frac{(\cos\vartheta_m \cos\tilde{\vartheta}_{j-N} + \sin\vartheta_m \sin\tilde{\vartheta}_{j-N})}{|\boldsymbol{x}_j - \boldsymbol{\xi}_m|^2} + 2\frac{(\boldsymbol{x}_j - \boldsymbol{\xi}_m)\cdot \boldsymbol{n}_j}{|\boldsymbol{x}_j - \boldsymbol{\xi}_m|^4} \left((\boldsymbol{x}_j - \boldsymbol{\xi}_m)\cdot(\cos\vartheta_m, \sin\vartheta_m)\right) \right],$$

$$j = \overline{N+1, N+M},\ m = \overline{1, N},$$

$$J_{M+j,3N+1} = \sum_{k=1}^{2N} c_k \frac{\partial\left(\partial_n G(\boldsymbol{\xi}_k, \boldsymbol{x}_j)\right)}{\partial \eta_{\text{int}}}$$

$$= \gamma \sum_{k=1}^{N} c_k r_k \left[-\frac{(\cos\vartheta_k \cos\tilde{\vartheta}_{j-N} + \sin\vartheta_k \sin\tilde{\vartheta}_{j-N})}{|\boldsymbol{x}_j - \boldsymbol{\xi}_k|^2} + 2\frac{(\boldsymbol{x}_j - \boldsymbol{\xi}_k)\cdot \boldsymbol{n}_j}{|\boldsymbol{x}_j - \boldsymbol{\xi}_k|^4} \left((\boldsymbol{x}_j - \boldsymbol{\xi}_k)\cdot(\cos\vartheta_k, \sin\vartheta_k)\right) \right],$$

$$j = \overline{N+1, N+M},$$

$$J_{M+j,3N+2} = \sum_{k=1}^{2N} c_k \frac{\partial\left(\partial_n G(\boldsymbol{\xi}_k, \boldsymbol{x}_j)\right)}{\partial \eta_{\text{ext}}}$$

$$= \gamma \sum_{k=N+1}^{2N} c_k R \left[-\frac{(\cos\vartheta_{k-N} \cos\tilde{\vartheta}_{j-N} + \sin\vartheta_{k-N} \sin\tilde{\vartheta}_{j-N})}{|\boldsymbol{x}_j - \boldsymbol{\xi}_k|^2} \right.$$

$$\left. + 2\frac{(\boldsymbol{x}_j - \boldsymbol{\xi}_k)\cdot \boldsymbol{n}_j}{|\boldsymbol{x}_j - \boldsymbol{\xi}_k|^4} \left((\boldsymbol{x}_j - \boldsymbol{\xi}_k)\cdot(\cos\vartheta_{k-N}, \sin\vartheta_{k-N})\right) \right], \quad j = \overline{N+1, N+M},$$

$$J_{M+j,3N+3} = \sum_{k=1}^{2N} c_k \frac{\partial\left(\partial_n G(\boldsymbol{\xi}_k, \boldsymbol{x}_j)\right)}{\partial X}$$

$$= \gamma \sum_{k=1}^{N} c_k \left[-\frac{\cos\tilde{\vartheta}_{j-N}}{|\boldsymbol{x}_j - \boldsymbol{\xi}_k|^2} + 2\frac{(\boldsymbol{x}_j - \boldsymbol{\xi}_k)\cdot \boldsymbol{n}_j}{|\boldsymbol{x}_j - \boldsymbol{\xi}_k|^4} (\boldsymbol{x}_j - \boldsymbol{\xi}_k)_x \right], \quad j = \overline{N+1, N+M},$$

$$J_{M+j,3N+4} = \sum_{k=1}^{2N} c_k \frac{\partial\left(\partial_n G(\boldsymbol{\xi}_k, \boldsymbol{x}_j)\right)}{\partial Y}$$

$$= \gamma \sum_{k=1}^{N} c_k \left[-\frac{\sin\tilde{\vartheta}_{j-N}}{|\boldsymbol{x}_j - \boldsymbol{\xi}_k|^2} + 2\frac{(\boldsymbol{x}_j - \boldsymbol{\xi}_k)\cdot \boldsymbol{n}_j}{|\boldsymbol{x}_j - \boldsymbol{\xi}_k|^4} (\boldsymbol{x}_j - \boldsymbol{\xi}_k)_y \right], \quad j = \overline{N+1, N+M},$$

$$F_{2M+N+1} = \sqrt{\lambda_1 \sum_{\ell=1}^{2N} c_\ell^2},$$

. . . . . .

$$J_{2M+N+1,m} = \frac{\partial}{\partial c_m}\sqrt{\lambda_1 \sum_{\ell=1}^{2N} c_\ell^2} = \sqrt{\lambda_1}\,\frac{c_m}{\sqrt{\sum_{\ell=1}^{2N} c_\ell^2}}, \quad m = \overline{1, 2N},$$

$$J_{2M+N+1,2N+m} = \frac{\partial}{\partial r_m}\sqrt{\lambda_1 \sum_{\ell=1}^{2N} c_\ell^2} = 0, \quad m = \overline{1,N},$$

$$J_{2M+N+1,3N+1} = \frac{\partial}{\partial \eta_{\text{int}}}\sqrt{\lambda_1 \sum_{\ell=1}^{2N} c_\ell^2} = 0, \quad J_{2M+N+1,3N+2} = \frac{\partial}{\partial \eta_{\text{ext}}}\sqrt{\lambda_1 \sum_{\ell=1}^{2N} c_\ell^2} = 0,$$

$$J_{2M+N+1,3N+3} = \frac{\partial}{\partial X}\sqrt{\lambda_1 \sum_{\ell=1}^{2N} c_\ell^2} = 0, \quad J_{2M+N+1,3N+4} = \frac{\partial}{\partial Y}\sqrt{\lambda_1 \sum_{\ell=1}^{2N} c_\ell^2} = 0,$$

$$F_{2M+N+2} = \sqrt{\lambda_2 \sum_{\ell=2}^{N} \left(r_\ell - r_{\ell-1}\right)^2},$$

. . . . . .

$$J_{2M+N+2,m} = \frac{\partial}{\partial c_m}\sqrt{\lambda_2 \sum_{\ell=2}^{N} \left(r_\ell - r_{\ell-1}\right)^2} = 0, \quad m = \overline{1,2N},$$

$$J_{2M+N+2,2N+1} = \frac{\partial}{\partial r_1}\sqrt{\lambda_2 \sum_{\ell=2}^{N} \left(r_\ell - r_{\ell-1}\right)^2} = -\sqrt{\lambda_2}\,\frac{(r_2 - r_1)}{\sqrt{\sum_{\ell=2}^{N} \left(r_\ell - r_{\ell-1}\right)^2}},$$

$$J_{2M+N+2,2N+m} = \frac{\partial}{\partial r_m}\sqrt{\lambda_2 \sum_{\ell=2}^{N} \left(r_\ell - r_{\ell-1}\right)^2} = \sqrt{\lambda_2}\,\frac{(2r_m - r_{m-1} - r_{m+1})}{\sqrt{\sum_{\ell=2}^{N} \left(r_\ell - r_{\ell-1}\right)^2}}, \quad m = \overline{2,N-1},$$

$$J_{2M+N+2,2N+N} = \frac{\partial}{\partial r_N}\sqrt{\lambda_2 \sum_{\ell=2}^{N} \left(r_\ell - r_{\ell-1}\right)^2} = \sqrt{\lambda_2}\,\frac{(r_N - r_{N-1})}{\sqrt{\sum_{\ell=2}^{N} \left(r_\ell - r_{\ell-1}\right)^2}},$$

$$J_{2M+N+2,3N+1} = \frac{\partial}{\partial \eta_{\text{int}}}\sqrt{\lambda_2 \sum_{\ell=2}^{N} \left(r_\ell - r_{\ell-1}\right)^2} = 0,$$

$$J_{2M+N+2,3N+2} = \frac{\partial}{\partial \eta_{\text{ext}}}\sqrt{\lambda_2 \sum_{\ell=2}^{N} \left(r_\ell - r_{\ell-1}\right)^2} = 0,$$

$$J_{2M+N+2,3N+3} = \frac{\partial}{\partial X}\sqrt{\lambda_2 \sum_{\ell=2}^{N} \left(r_\ell - r_{\ell-1}\right)^2} = 0,$$

TABLE 1. Example 1: CPU times in seconds with number of iterations, with and without providing the Jacobian, no noise and no regularization.

`niter`	With Jacobian	Without Jacobian
10	0.0748	0.8594
20	0.1370	1.3729
50	0.3458	3.3686
100	0.6756	6.4056
200	1.1580	12.478
500	2.3014	32.169
1000	4.9697	82.788

$$J_{2M+N+2,3N+4} = \frac{\partial}{\partial Y}\sqrt{\lambda_2 \sum_{\ell=2}^{N} \left(r_\ell - r_{\ell-1}\right)^2} = 0.$$

5. Numerical examples

In all examples considered in this study we have taken the outer boundary $\partial\Omega_2$ to be a circle of radius $R = 1$, whilst the choice of the regularization parameters λ_1 and λ_2 is based on trial and error. However, one would expect that more sophisticated methods of selecting the regularization parameters will lead to even better reconstructions, see e.g. [2,5]. Nonetheless, this is beyond the scope of this investigation since one of our main aims herein is to emphasize the fact that both regularizing terms occurring in functional (4.1) are important and each yields a stabilised/regularized solution to the missing inner boundary that is exempted from high oscillations.

5.1. **Example 1.** Here we consider reconstructing a circular rigid inclusion with boundary $\partial\Omega_1$ of radius 0.5 in the case where $X = Y = 0$ and $\alpha = 1$ in (2.1d). The Dirichlet data (2.1e) on $\partial\Omega_2$ is taken as [13],

$$u(1,\vartheta) = f(\vartheta) = \mathrm{e}^{-\cos^2\vartheta}, \quad \vartheta \in [0, 2\pi). \tag{5.1}$$

The Neumann data (2.1f) is simulated by solving the direct mixed well-posed boundary value problem (2.1a), (2.1b) and (5.1), using the MFS with $M = N = 400$ and $\eta_{\text{int}} = 0.8, \eta_{\text{ext}} = 1.2$. In order to avoid committing an inverse crime, the inverse solver is applied using $N = 56, M = 64$. We choose the initial vector of unknowns $\mathbf{x}_0 = (\boldsymbol{c}_0, \boldsymbol{r}_0, \eta^0_{\text{int}}, \eta^0_{\text{ext}}, X_0, Y_0)^{\mathrm{T}} = (\mathbf{0}, \mathbf{0.1}, 0.3, 2, -0.3, 0.25)^{\mathrm{T}}$. In Table 1 we present the CPU times required for the above parameters for different numbers of iterations when providing and when not providing the Jacobian. The savings when providing the Jacobian are spectacular.

In Figure 2 we present the reduction of the residual functional (4.1) after 100 iterations with no noise and no regularization when providing the Jacobian and when not providing the Jacobian. As can be observed, when providing the Jacobian the residual decreases much faster.

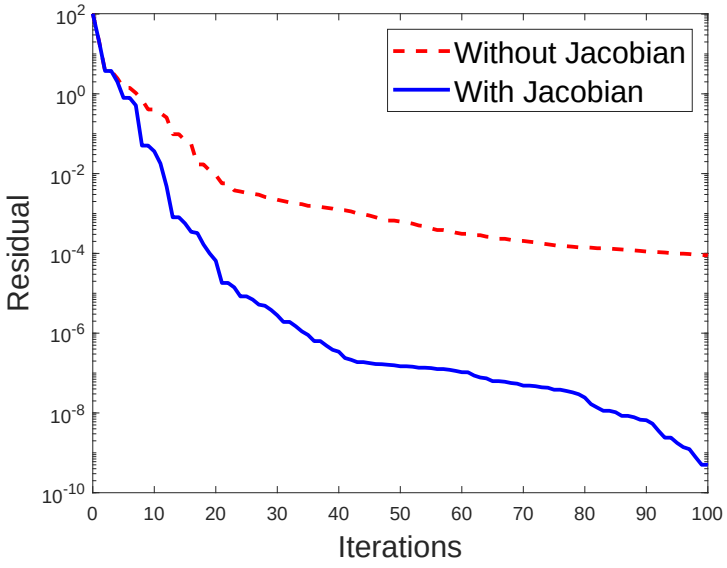

FIGURE 2. Example 1: Residual functional (4.1) with number of iterations, no noise and no regularization.

In Figure 3 we present the results obtained for different numbers of iterations, with no noise and no regularization, i.e. $\lambda_1 = \lambda_2 = 0$. It can be seen that the solution becomes accurate after about 20 iterations.
In Figures 4 and 5 we present the reconstructed curves with noise level of 10% after 1000 iterations and various regularization parameters λ_1 when $\lambda_2 = 0$, and λ_2 when $\lambda_1 = 0$, respectively. From these figures it can be seen that the inclusion of regularization, either with λ_1 or λ_2, yields stable numerical solutions. In Figure 5 it is clear that as λ_2 increases, the reconstruction tends to a circle (of radius 0.5), due to the fact that the distribution of points $(\mathbf{x}_k)_{k=\overline{1,N}}$ that minimize the distance between them (which is what λ_2 penalises) is an equally–spaced distribution of points over a circumference. In this way, a high λ_2 seems to be an advantage in the case of circular voids. On the contrary, this a drawback for other domains, as will be further illustrated later in Figure 8 for the (non–circular) bean–shaped void (5.2). Moreover, it seems that regularizing the boundary $\partial\Omega_1$ is less sensitive to the choice of the regularization parameter λ_2 (in between 10^{-2} and 10^2) than is regularizing the solution u (i.e. the vector of coefficients $\boldsymbol{c}$) through the regularization parameter $\lambda_1 = 10^{-5}$.

5.2. **Example 2.** We consider a bean-shaped rigid inclusion whose boundary $\partial\Omega_1$ is described by $X = 0.2$, $Y = 0.3$, and the radial parametrization

$$r(\vartheta) = 0.6 \left(\frac{0.5 + 0.4\cos(\vartheta) + 0.1\sin(2\vartheta)}{1 + 0.7\cos(\vartheta)} \right), \quad \vartheta \in [0, 2\pi), \tag{5.2}$$

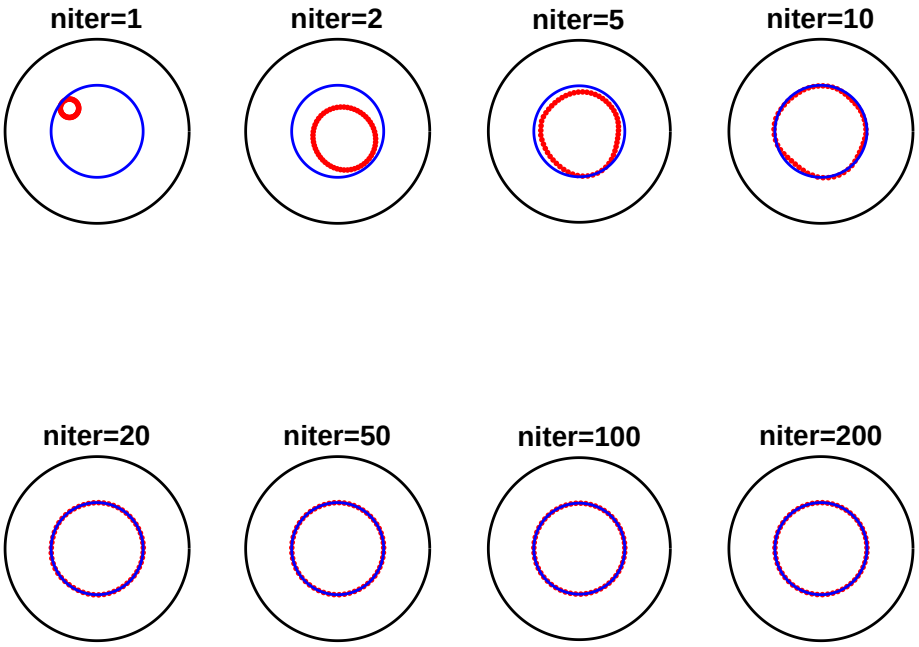

FIGURE 3. Example 1: Results for various numbers of iterations, no noise and no regularization.

in the case of $\alpha = 1$ in (2.1d). This example, which was also considered in [13], is more difficult than Example 1 because of the presence of a sharp cusp-like portion mimicking a re-entrant corner. The Neumann data (2.1f) is simulated by solving the direct mixed well-posed boundary value problem (2.1a), (2.1b) and (5.1), when $\partial\Omega_1$ is given by (5.2), using the MFS with $M = N = 400$ and $\eta_{\rm int} = 0.8, \eta_{\rm ext} = 1.2$. In order to avoid committing an inverse crime, the inverse solver is applied using $N = 56, M = 64$. We choose the initial vector of unknowns $\mathbf{x}_0 = (\boldsymbol{c}_0, \boldsymbol{r}_0, \eta^0_{\rm int}, \eta^0_{\rm ext}, X_0, Y_0)^{\rm T} = (\mathbf{0}, \mathbf{0.1}, 0.3, 2, 0.1, 0)^{\rm T}$.

In Figure 6 we present the results obtained for different numbers of iterations, with no noise and no regularization, i.e. $\lambda_1 = \lambda_2 = 0$. From these figures it can be seen that the solution becomes quite accurate after about 100 iterations.

In Figures 7 and 8 we present the reconstructed curves with noise level of 5% after 1000 iterations and various regularization parameters λ_1 when $\lambda_2 = 0$, and λ_2 when $\lambda_1 = 0$, respectively. From these figures it can be seen that the inclusion of regularization, either with λ_1 or λ_2, yields stable numerical solutions.

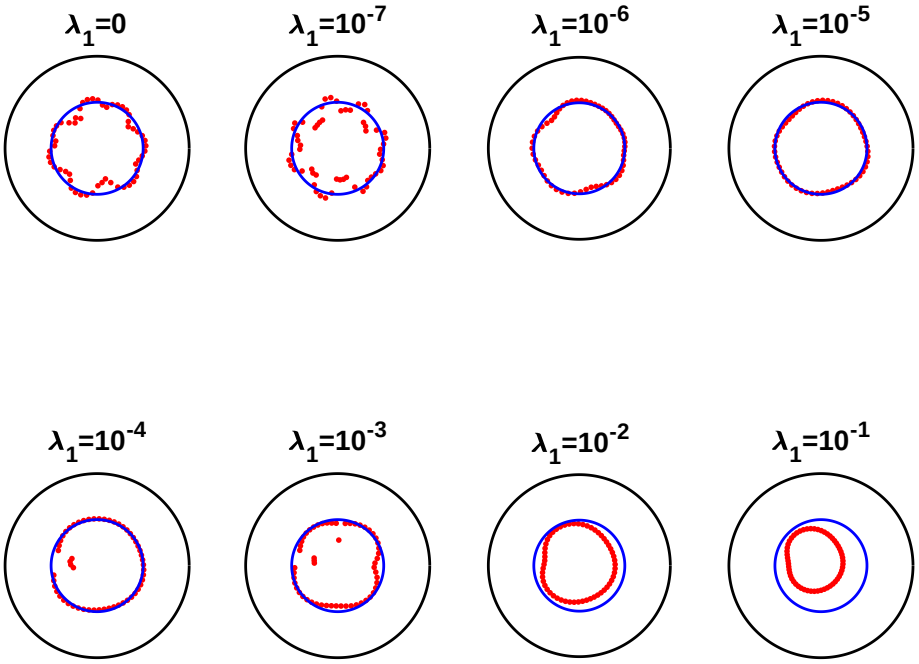

FIGURE 4. Example 1: Results for noise $p = 10\%$ and regularization with λ_1.

5.3. **Example 3.** We consider an example for which the exact solution is known. Here we consider reconstructing a circular cavity (i.e. $\alpha = 0$ in (2.1d)) centred at the origin $(X, Y) = (0, 0)$. In particular, we consider

$$\Omega_1 = \left\{(x, y) \in \mathbb{R}^2 : x^2 + y^2 < R_0^2 < 1\right\}, \quad \Omega_2 = \left\{(x, y) \in \mathbb{R}^2 : x^2 + y^2 < 1\right\} \tag{5.3}$$

and

$$u(x, y) = \frac{x}{R_0^2} + \frac{x}{x^2 + y^2}. \tag{5.4}$$

For any $0 < R_0 < 1$, the function u satisfies equations (2.1a), (2.1c), (2.1e) and (2.1f), with

$$f(x, y) = x\left(\frac{1}{R_0^2} + 1\right) \quad \text{and} \quad g(x, y) = x\left(\frac{1}{R_0^2} - 1\right), \quad (x, y) \in \partial\Omega_2. \tag{5.5}$$

Note that the compatibility condition (2.2) on the Neumann flux data g is automatically satisfied.

In our numerical experiments we consider $R_0 = 0.5$. We choose the initial vector of unknowns $\mathbf{x}_0 = (\boldsymbol{c}_0, \boldsymbol{r}_0, \eta^0_{\text{int}}, \eta^0_{\text{ext}}, X_0, Y_0)^{\text{T}} = (\mathbf{0}, \mathbf{0.1}, 0.1, 2, -0.1, 0.5)^{\text{T}}$.

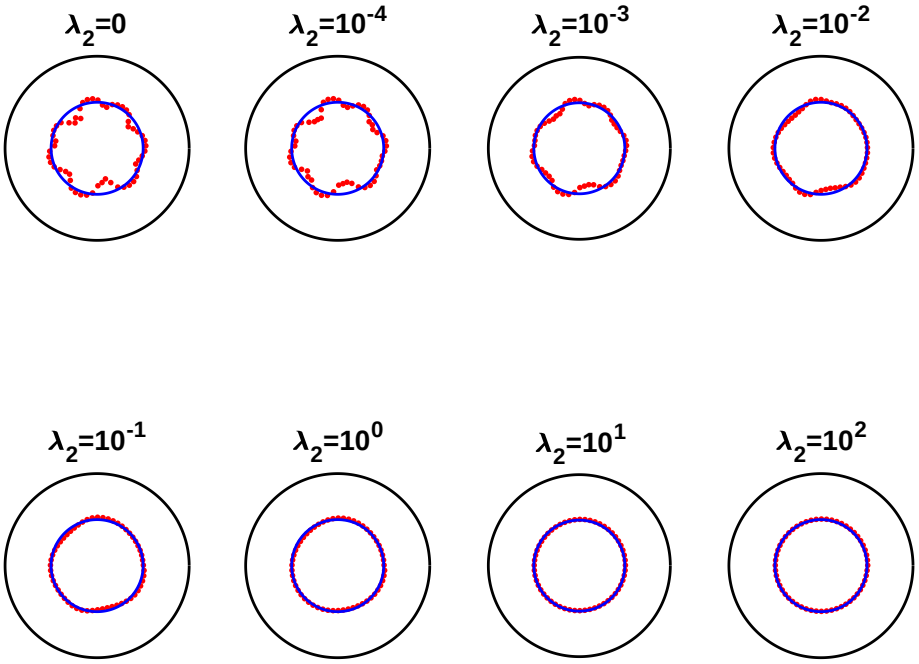

FIGURE 5. Example 1: Results for noise $p = 10\%$ and regularization with λ_2.

In Figure 9 we present the results obtained for different numbers of iterations, with no noise and no regularization, i.e. $\lambda_1 = \lambda_2 = 0$. From these figures it can be seen that the solution becomes quite accurate after about 20 iterations.
In Figures 10 and 11 we present the reconstructed curves with noise level of 5% after 1000 iterations and various regularization parameters λ_1 when $\lambda_2 = 0$, and λ_2 when $\lambda_1 = 0$, respectively. From these figures it can be seen that the inclusion of regularization, either with λ_1 or λ_2, yields stable numerical solutions.

5.4. **Example 4.** We consider a bean-shaped cavity (i.e. $\alpha = 0$ in (2.1d)) whose boundary $\partial\Omega_1$ is described by $X = 0.2$, $Y = 0.3$, and the radial parametrization (5.2). The numerical details are the same as those of Example 2, except for the initial guess which is taken $\mathbf{x}_0 = (\boldsymbol{c}_0, \boldsymbol{r}_0, \eta^0_{\rm int}, \eta^0_{\rm ext}, X_0, Y_0)^{\rm T} = (\mathbf{0}, \mathbf{0.25}, 0.3, 2, -0.2, -0.2)^{\rm T}$.
In Figure 12 we present the results obtained for different numbers of iterations, with no noise and no regularization, i.e. $\lambda_1 = \lambda_2 = 0$. From these figures it can be seen that the solution becomes quite accurate after about 1000 iterations.

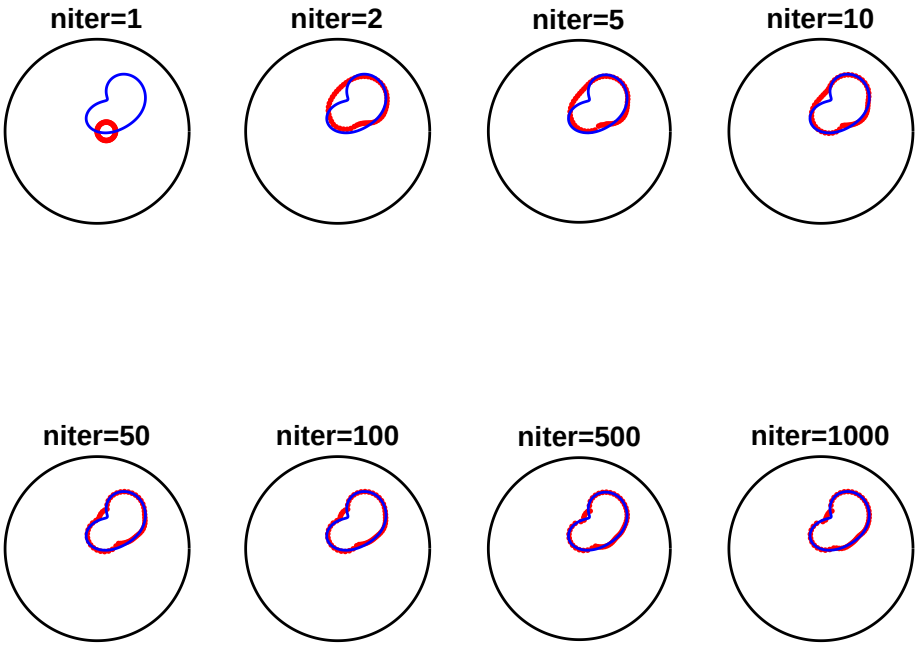

FIGURE 6. Example 2: Results for various numbers of iterations, no noise and no regularization.

In Figures 13 and 14 we present the reconstructed curves with noise level of 5% after 1000 iterations and various regularization parameters λ_1 when $\lambda_2 = 0$, and λ_2 when $\lambda_1 = 0$, respectively. From these figures it can be seen that the inclusion of regularization, either with λ_1 or λ_2, yields stable numerical solutions.

6. Extension to multiple voids

We now extend the MFS formulation for one void, described in Sections 3 and 4, to the case of two voids given by

$$\Delta u = 0 \quad \text{in } \Omega, \tag{6.1a}$$

subject to

$$u = f \quad \text{on } \partial\Omega_2, \tag{6.1b}$$

$$\partial_n u = g \quad \text{on } \partial\Omega_2, \tag{6.1c}$$

$$\alpha_1 u + (1-\alpha_1)\partial_n u = 0 \quad \text{on } \partial\Omega_1^a, \quad \text{where} \quad \alpha_1 \in \{0,1\}, \tag{6.1d}$$

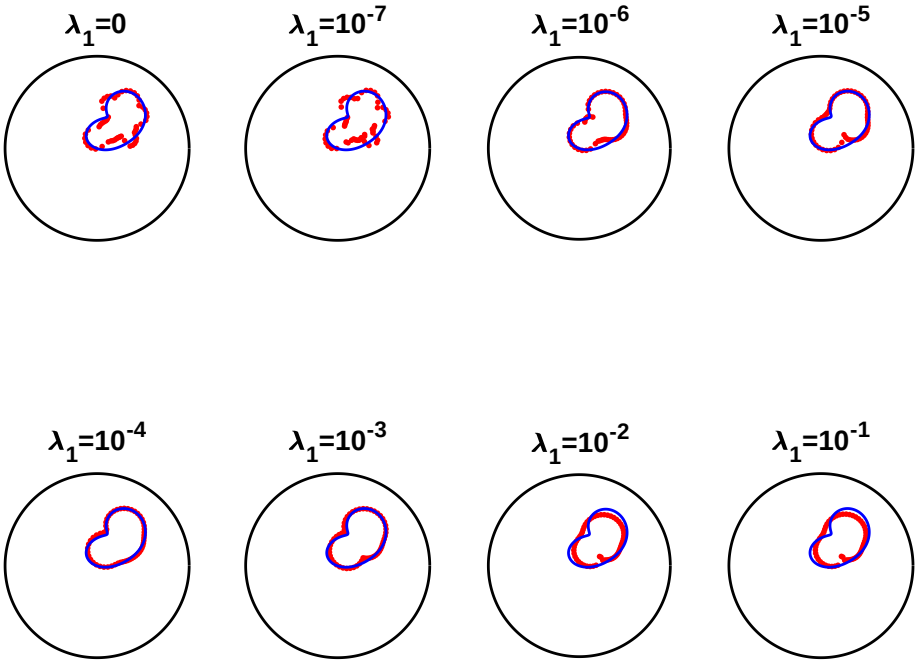

FIGURE 7. Example 2: Results for noise $p = 5\%$ and regularization with λ_1.

and

$$\alpha_2 u + (1-\alpha_2)\partial_n u = 0 \quad \text{on } \partial\Omega_1^b, \quad \text{where} \quad \alpha_2 \in \{0,1\}. \tag{6.1e}$$

Here Ω_1^a and Ω_1^b are two disjoint voids, such that $\Omega_1^a \cup \Omega_1^b = \Omega_1$ and $\overline{\Omega}_1^a \cap \overline{\Omega}_1^b = \emptyset$, see Figure 1.

The MFS approximation of the solution of inverse boundary value problem (6.1) is

$$u_N(\boldsymbol{c}, \boldsymbol{\xi}; \boldsymbol{x}) = \sum_{k=1}^{3N} c_k \, G(\boldsymbol{\xi}_k, \boldsymbol{x}), \quad \boldsymbol{x} \in \overline{\Omega}. \tag{6.2}$$

In this case $3N$ sources $(\boldsymbol{\xi}_k)_{k=\overline{1,3N}}$ are placed outside Ω, that is in $\Omega_1 \cup \left(\mathbb{R}^2 \backslash \bar{\Omega}_2\right)$. The first N sources $(\boldsymbol{\xi}_k)_{k=\overline{1,N}}$ are placed in Ω_1^a on a pseudo–boundary $\partial\Omega_1^{a\prime}$ similar to $\partial\Omega_1^a$. The next N sources $(\boldsymbol{\xi}_k)_{k=\overline{N+1,2N}}$ are placed in Ω_1^b on a pseudo–boundary $\partial\Omega_1^{b\prime}$ similar to $\partial\Omega_1^b$. Finally, the remaining N sources $(\boldsymbol{\xi}_k)_{k=\overline{2N+1,3N}}$ are placed in $\mathbb{R}^2 \backslash \overline{\Omega}_2$ on a pseudo–boundary $\partial\Omega_2'$ similar (dilation) to $\partial\Omega_2$. Note that the first two pseudo–boundaries are contractions with unknown contraction coefficients $\eta_{\text{int}}^a \in (0,1)$ and $\eta_{\text{int}}^b \in (0,1)$, respectively, while the third pseudo–boundary is a dilation with

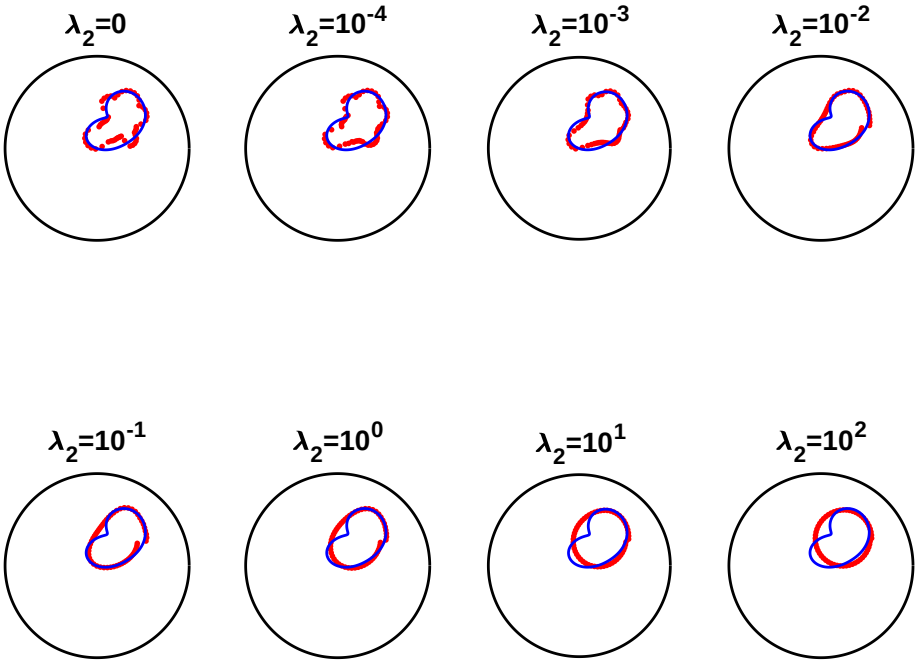

FIGURE 8. Example 2: Results for noise $p = 5\%$ and regularization with λ_2.

contraction coefficient $\eta_{\text{ext}} \in (1, S)$ with $S > 1$ prescribed.

We assume that the unknown boundaries $\partial\Omega_1^a$ and $\partial\Omega_1^b$ are a smooth, star–like curves with respect to their centres which have unknown coordinates (X^a, Y^a) and (X^b, Y^b), respectively. Their equations in polar coordinates are thus

$$(x, y)=(X^a + r^a(\vartheta)\cos\vartheta, Y^a + r^a(\vartheta)\sin\vartheta) \text{ and } (x, y)=\big(X^b + r^b(\vartheta)\cos\vartheta, Y^b + r^b(\vartheta)\sin\vartheta\big)\,, \quad (6.3)$$

$\vartheta \in [0, 2\pi)$, respectively, where r^a and r^b are smooth $2\pi-$periodic functions.

Using the notation

$$r_k = r_k^a = r^a(\vartheta_k), \quad r_{k+N} = r_k^b = r^b(\vartheta_k), \qquad k = \overline{1, N}, \quad (6.4)$$

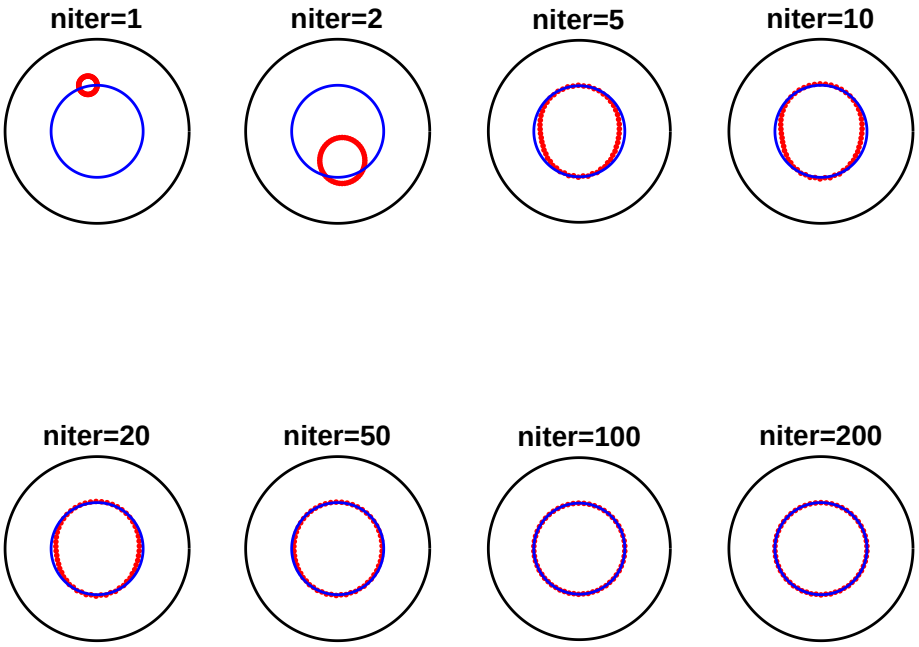

FIGURE 9. Example 3: Results for various numbers of iterations, no noise and no regularization.

the sources are defined as follows:

$$\begin{aligned} \boldsymbol{\xi}_k &= (X^a, Y^a) + \eta^a_{\text{int}}\, r^a_k\, (\cos\vartheta_k, \sin\vartheta_k)\,, \\ \boldsymbol{\xi}_{N+k} &= (X^b, Y^b) + \eta^b_{\text{int}}\, r^b_{N+k}\, (\cos\vartheta_k, \sin\vartheta_k)\,, \\ \boldsymbol{\xi}_{2N+k} &= \eta_{\text{ext}} R(\cos\vartheta_k, \sin\vartheta_k), \quad k = \overline{1,N}, \end{aligned} \tag{6.5}$$

where $\vartheta_k = \frac{2\pi(k-1)}{N}$, $k = \overline{1,N}$. In addition to the sources, we define $2N+M$ boundary collocation points $(\boldsymbol{x}_\ell)_{\ell=\overline{1,2N+M}}$ as follows:

$$\begin{aligned} \boldsymbol{x}_k &= (X^a, Y^a) + r^a_k\, (\cos\vartheta_k, \sin\vartheta_k)\,, \\ \boldsymbol{x}_{N+k} &= (X^b, Y^b) + r^b_{N+k}\, (\cos\vartheta_k, \sin\vartheta_k)\,, \quad k = \overline{1,N}, \\ \boldsymbol{x}_{2N+\ell} &= R\,(\cos\tilde{\vartheta}_\ell, \sin\tilde{\vartheta}_\ell), \quad \ell = \overline{1,M}, \end{aligned} \tag{6.6}$$

where $\tilde{\vartheta}_\ell = \frac{2\pi(\ell-1)}{M}$, $\ell = \overline{1,M}$.

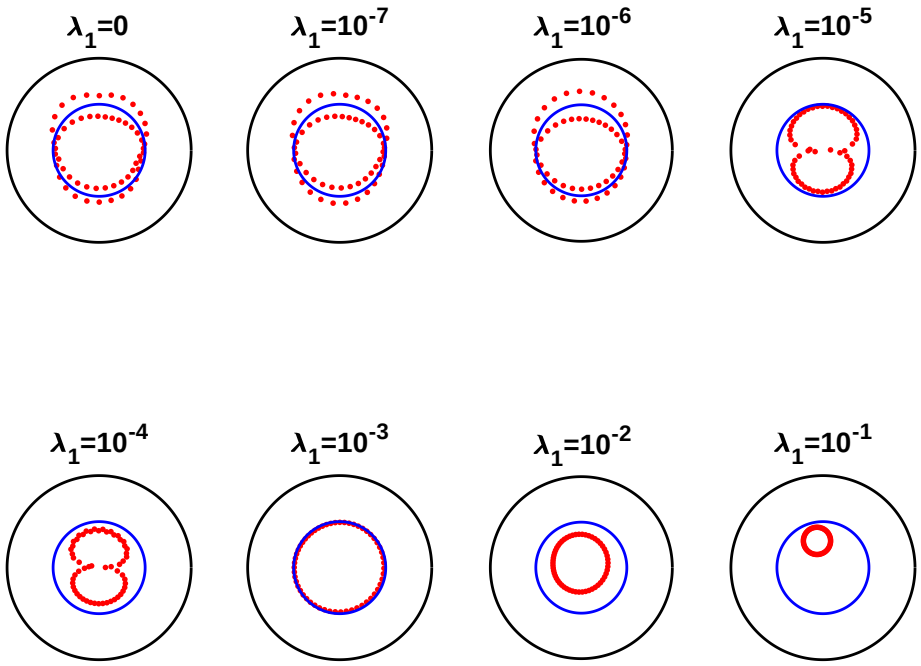

FIGURE 10. Example 3: Results for noise $p = 5\%$ and regularization with λ_1.

In the MFS formulation for the solution of inverse boundary value problem (6.1) we have the following unknowns:

- The coefficients $(c_k)_{k=\overline{1,3N}}$ in (6.2),
- the radii $(r_k^a)_{k=\overline{1,N}}$, $\left(r_k^b\right)_{k=\overline{1,N}}$ in (6.4),
- the contraction and dilation coefficients $\eta_{\text{int}}^a, \eta_{\text{int}}^b$ and η_{ext}, and
- the centre coordinates $(X^a, Y^a), (X^b, Y^b)$.

The unknowns listed above are determined by imposing the boundary conditions (6.1b)–(6.1e) in a least-squares sense by minimizing the functional

$$S(\boldsymbol{c}, \boldsymbol{r}^a, \boldsymbol{r}^b, \boldsymbol{\eta}, \boldsymbol{C}) := \sum_{j=2N+1}^{2N+M} \left[u_N(\boldsymbol{c}, \boldsymbol{\xi}; \boldsymbol{x}_j) - f(\boldsymbol{x}_j)\right]^2 + \sum_{j=2N+1}^{2N+M} \left[\partial_n u_N(\boldsymbol{c}, \boldsymbol{\xi}; \boldsymbol{x}_j) - g^\varepsilon(\boldsymbol{x}_j)\right]^2$$

$$+ \sum_{j=1}^{N} \left[\alpha_1 u_N(\boldsymbol{c}, \boldsymbol{\xi}; \boldsymbol{x}_j) + (1-\alpha_1)\partial_n u_N(\boldsymbol{c}, \boldsymbol{\xi}; \boldsymbol{x}_j)\right]^2 + \sum_{j=N+1}^{2N} \left[\alpha_2 u_N(\boldsymbol{c}, \boldsymbol{\xi}; \boldsymbol{x}_j) + (1-\alpha_2)\partial_n u_N(\boldsymbol{c}, \boldsymbol{\xi}; \boldsymbol{x}_j)\right]^2$$

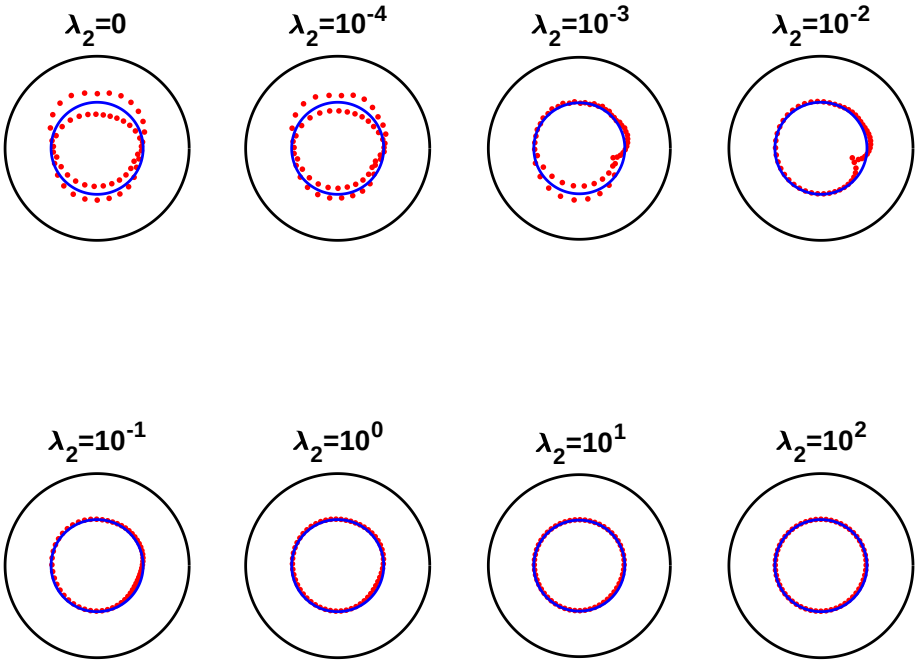

FIGURE 11. Example 3: Results for noise $p = 5\%$ and regularization with λ_2.

$$+ \lambda_1 |\boldsymbol{c}|^2 + \lambda_2^a \sum_{\ell=2}^{N} \left(r_\ell^a - r_{\ell-1}^a\right)^2 + \lambda_2^b \sum_{\ell=2}^{N} \left(r_\ell^b - r_{\ell-1}^b\right)^2, \tag{6.7}$$

where $\lambda_1, \lambda_2^a, \lambda_2^b \geq 0$ are regularization parameters to be prescribed, $\boldsymbol{c} = [c_1, c_2, \ldots, c_{3N}]^{\mathrm{T}}$, $\boldsymbol{r}^a = [r_1^a, r_2^a, \ldots, r_N^a]^{\mathrm{T}}$, $\boldsymbol{r}^b = [r_1^b, r_2^b, \ldots, r_N^b]^{\mathrm{T}}$, $\boldsymbol{\eta} = [\eta_{\mathrm{int}}^a, \eta_{\mathrm{int}}^b, \eta_{\mathrm{ext}}]^{\mathrm{T}}$ and $\boldsymbol{C} = [X^a, Y^a, X^b, Y^b]^{\mathrm{T}}$. The number of unknowns is $5N + 7$ and the number of boundary collocation equations $2N + 2M$, and thus we need to take $2M \geq 3N + 7$.

6.1. **Derivation of Jacobian.** In the implementation we need to provide `lsqnonlin` with the following information (for simplicity we only consider the case $\alpha_1 = \alpha_2 = 1$ in (6.1d) and (6.1e), respectively):

$$F_j = \sum_{k=1}^{3N} c_k \, G(\boldsymbol{\xi}_k, \boldsymbol{x}_j) = \gamma \sum_{k=1}^{N} c_k \log \sqrt{\left(r_j \cos\vartheta_j - \eta_{\mathrm{int}}^a r_k \cos\vartheta_k\right)^2 + \left(r_j \sin\vartheta_j - \eta_{\mathrm{int}}^a r_k \sin\vartheta_k\right)^2}$$

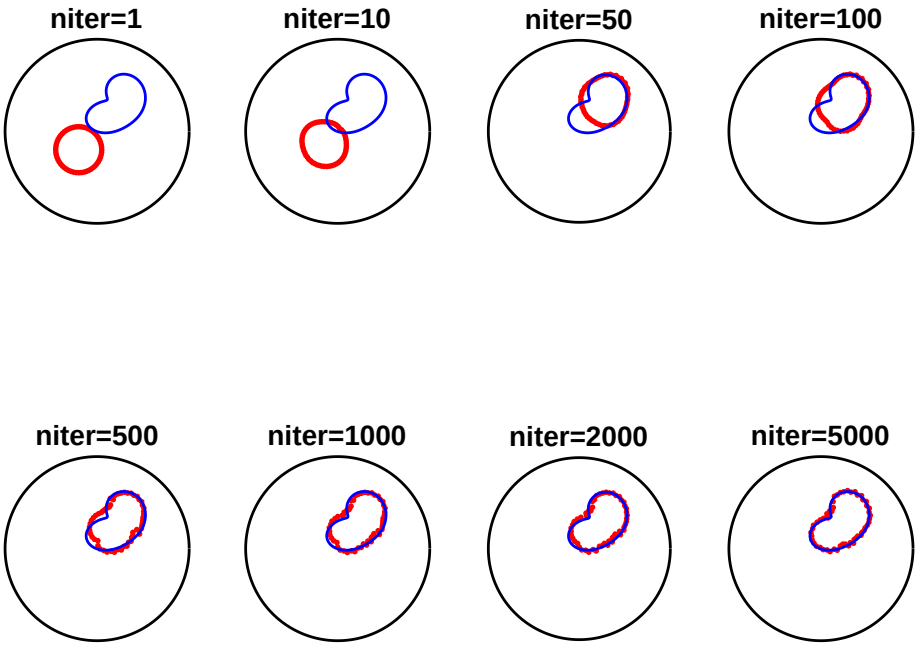

FIGURE 12. Example 4: Results for various numbers of iterations, no noise and no regularization.

$$+\gamma \sum_{k=N+1}^{2N} c_k \log \sqrt{\left(X^a + r_j \cos\vartheta_j - X^b - \eta_{\text{int}}^b r_k \cos\vartheta_k\right)^2 + \left(Y^a + r_j \sin\vartheta_j - Y^b - \eta_{\text{int}}^b r_k \sin\vartheta_k\right)^2}$$

$$+\gamma \sum_{k=2N+1}^{3N} c_k \log \sqrt{\left(X^a + r_j \cos\vartheta_j - \eta_{\text{ext}} R \cos\vartheta_{k-2N}\right)^2 + \left(Y^a + r_j \sin\vartheta_j - \eta_{\text{ext}} R \sin\vartheta_{k-2N}\right)^2},$$

$j = \overline{1, N}$,

. . . . . .

$$J_{j,m} = G(\boldsymbol{\xi}_m, \boldsymbol{x}_j), \quad j = \overline{1, N},\ m = \overline{1, 3N},$$

$$J_{j,3N+m} = \frac{\partial}{\partial r_m} \sum_{k=1}^{3N} c_k\, G(\boldsymbol{\xi}_k, \boldsymbol{x}_j)$$

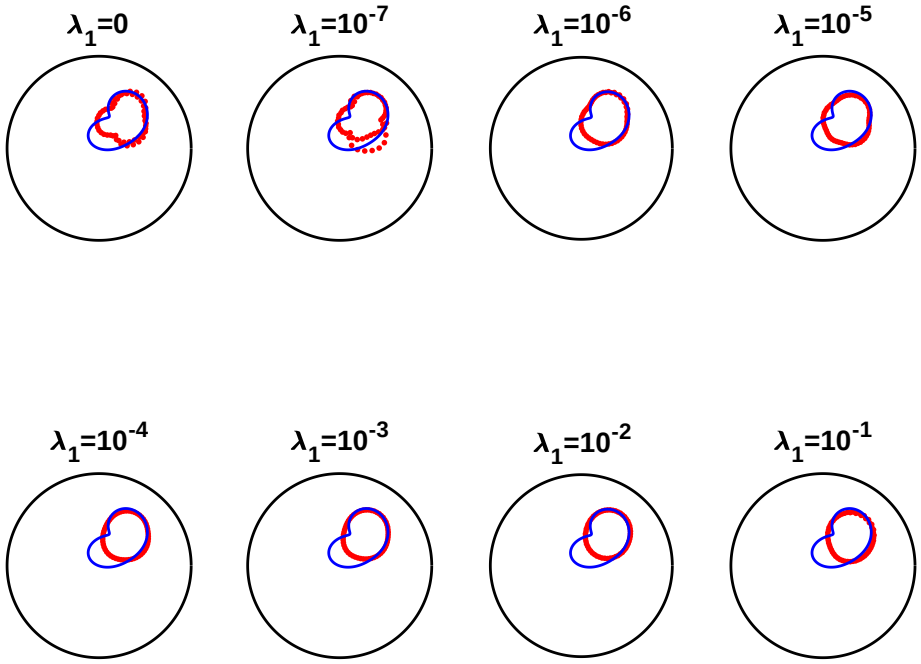

FIGURE 13. Example 4: Results for noise $p = 5\%$ and regularization with λ_1.

$$= -\gamma\eta^a_{\rm int}c_m\frac{(\boldsymbol{x}_j-\boldsymbol{\xi}_m)\cdot(\cos\vartheta_m,\sin\vartheta_m)}{|\boldsymbol{x}_j-\boldsymbol{\xi}_m|^2},\quad m\neq j,\quad j=\overline{1,N},\ m=\overline{1,N},$$

$$J_{m,3N+m}=\frac{\partial}{\partial r_m}\sum_{k=1}^{3N}c_k\,G(\boldsymbol{\xi}_k,\boldsymbol{x}_j)$$

$$= -\gamma\eta^a_{\rm int}c_m\frac{(\boldsymbol{x}_m-\boldsymbol{\xi}_m)\cdot(\cos\vartheta_m,\sin\vartheta_m)}{|\boldsymbol{x}_m-\boldsymbol{\xi}_m|^2}+\gamma\sum_{k=1}^{3N}c_k\frac{(\boldsymbol{x}_m-\boldsymbol{\xi}_k)\cdot(\cos\vartheta_m,\sin\vartheta_m)}{|\boldsymbol{x}_m-\boldsymbol{\xi}_k|^2},\quad m=\overline{1,N},$$

$$J_{j,3N+m}=\frac{\partial}{\partial r_m}\sum_{k=1}^{3N}c_k\,G(\boldsymbol{\xi}_k,\boldsymbol{x}_j)$$

$$= -\gamma\eta^b_{\rm int}c_m\frac{(\boldsymbol{x}_j-\boldsymbol{\xi}_m)\cdot(\cos\vartheta_{m-N},\sin\vartheta_{m-N})}{|\boldsymbol{x}_j-\boldsymbol{\xi}_m|^2},\quad j=\overline{1,N},\ m=\overline{N+1,2N},$$

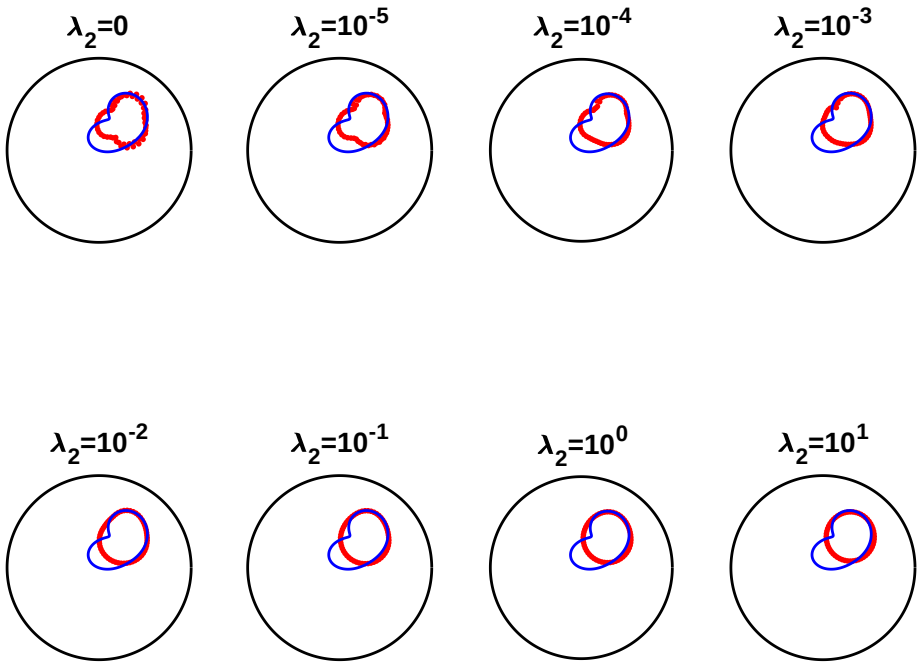

FIGURE 14. Example 4: Results for noise $p = 5\%$ and regularization with λ_2.

$$J_{j,5N+1} = \sum_{k=1}^{3N} c_k \frac{\partial G(\boldsymbol{\xi}_k, \boldsymbol{x}_j)}{\partial \eta^a_{\text{int}}} = -\gamma \sum_{k=1}^{N} c_k r_k \frac{(\boldsymbol{x}_j - \boldsymbol{\xi}_k) \cdot (\cos\vartheta_k, \sin\vartheta_k)}{|\boldsymbol{x}_j - \boldsymbol{\xi}_k|^2}, \quad j = \overline{1, N},$$

$$J_{j,5N+2} = \sum_{k=1}^{3N} c_k \frac{\partial G(\boldsymbol{\xi}_k, \boldsymbol{x}_j)}{\partial \eta^b_{\text{int}}} = -\gamma \sum_{k=N+1}^{2N} c_k r_k \frac{(\boldsymbol{x}_j - \boldsymbol{\xi}_k) \cdot (\cos\vartheta_k, \sin\vartheta_k)}{|\boldsymbol{x}_j - \boldsymbol{\xi}_k|^2}, \quad j = \overline{1, N},$$

$$J_{j,5N+3} = \sum_{k=1}^{3N} c_k \frac{\partial G(\boldsymbol{\xi}_k, \boldsymbol{x}_j)}{\partial \eta_{\text{ext}}} = -\gamma \sum_{k=2N+1}^{3N} c_k R \frac{(\boldsymbol{x}_j - \boldsymbol{\xi}_k) \cdot (\cos\vartheta_{k-2N}, \sin\vartheta_{k-2N})}{|\boldsymbol{x}_j - \boldsymbol{\xi}_k|^2}, \quad j = \overline{1, N},$$

$$J_{j,5N+4} = \sum_{k=1}^{2N} c_k \frac{\partial G(\boldsymbol{\xi}_k, \boldsymbol{x}_j)}{\partial X^a} = \gamma \sum_{k=N+1}^{3N} c_k \frac{(\boldsymbol{x}_j - \boldsymbol{\xi}_k)_x}{|\boldsymbol{x}_j - \boldsymbol{\xi}_k|^2}, \quad j = \overline{1, N},$$

$$J_{j,5N+5} = \sum_{k=1}^{2N} c_k \frac{\partial G(\boldsymbol{\xi}_k, \boldsymbol{x}_j)}{\partial Y^a} = \gamma \sum_{k=N+1}^{3N} c_k \frac{(\boldsymbol{x}_j - \boldsymbol{\xi}_k)_y}{|\boldsymbol{x}_j - \boldsymbol{\xi}_k|^2}, \quad j = \overline{1, N},$$

$$J_{j,5N+6} = \sum_{k=1}^{2N} c_k \frac{\partial G(\boldsymbol{\xi}_k, \boldsymbol{x}_j)}{\partial X^b} = -\gamma \sum_{k=N+1}^{2N} c_k \frac{(\boldsymbol{x}_j - \boldsymbol{\xi}_k)_x}{|\boldsymbol{x}_j - \boldsymbol{\xi}_k|^2}, \quad j = \overline{1, N},$$

$$J_{j,5N+7} = \sum_{k=1}^{2N} c_k \frac{\partial G(\boldsymbol{\xi}_k, \boldsymbol{x}_j)}{\partial Y^b} = -\gamma \sum_{k=N+1}^{2N} c_k \frac{(\boldsymbol{x}_j - \boldsymbol{\xi}_k)_y}{|\boldsymbol{x}_j - \boldsymbol{\xi}_k|^2}, \quad j = \overline{1, N},$$

$$F_j = \sum_{k=1}^{3N} c_k \, G(\boldsymbol{\xi}_k, \boldsymbol{x}_j)$$

$$= \gamma \sum_{k=1}^{N} c_k \log \sqrt{(X^b + r_j \cos\vartheta_j - X^a - \eta_{\text{int}}^a r_k \cos\vartheta_k)^2 + (Y^b + r_j \sin\vartheta_j - Y^a - \eta_{\text{int}}^a r_k \sin\vartheta_k)^2}$$

$$+\gamma \sum_{k=N+1}^{2N} c_k \log \sqrt{\left(r_j \cos\vartheta_j - \eta_{\text{int}}^b r_k \cos\vartheta_k\right)^2 + \left(r_j \sin\vartheta_j - \eta_{\text{int}}^b r_k \sin\vartheta_k\right)^2}$$

$$+\gamma \sum_{k=2N+1}^{3N} c_k \log \sqrt{(X^b + r_j \cos\vartheta_j - \eta_{\text{ext}} R \cos\vartheta_{k-2N})^2 + (Y^b + r_j \sin\vartheta_j - \eta_{\text{ext}} R \sin\vartheta_{k-2N})^2},$$

$j = \overline{N+1, 2N}$,

. . . . . .

$$J_{j,m} = G(\boldsymbol{\xi}_m, \boldsymbol{x}_j), \quad j = \overline{N+1, 2N}, \ m = \overline{1, 3N},$$

$$J_{j,3N+m} = \frac{\partial}{\partial r_m} \sum_{k=1}^{3N} c_k \, G(\boldsymbol{\xi}_k, \boldsymbol{x}_j)$$

$$= -\gamma \eta_{\text{int}}^a c_m \frac{(\boldsymbol{x}_j - \boldsymbol{\xi}_m) \cdot (\cos\vartheta_m, \sin\vartheta_m)}{|\boldsymbol{x}_j - \boldsymbol{\xi}_m|^2}, \quad j = \overline{N+1, 2N}, \ m = \overline{1, N},$$

$$J_{j,3N+m} = \frac{\partial}{\partial r_m} \sum_{k=1}^{3N} c_k \, G(\boldsymbol{\xi}_k, \boldsymbol{x}_j)$$

$$= -\gamma \eta_{\text{int}}^b c_m \frac{(\boldsymbol{x}_j - \boldsymbol{\xi}_m) \cdot (\cos\vartheta_{m-N}, \sin\vartheta_{m-N})}{|\boldsymbol{x}_j - \boldsymbol{\xi}_m|^2}, \quad m \neq j, \quad j = \overline{N+1, 2N}, \ m = \overline{N+1, 2N},$$

$$J_{m,3N+m} = \frac{\partial}{\partial r_m} \sum_{k=1}^{3N} c_k \, G(\boldsymbol{\xi}_k, \boldsymbol{x}_j)$$

$$= -\gamma \eta_{\text{int}}^b c_m \frac{(\boldsymbol{x}_m - \boldsymbol{\xi}_m) \cdot (\cos\vartheta_{m-N}, \sin\vartheta_{m-N})}{|\boldsymbol{x}_m - \boldsymbol{\xi}_m|^2} + \gamma \sum_{k=1}^{N} c_k \frac{(\boldsymbol{x}_m - \boldsymbol{\xi}_k) \cdot (\cos\vartheta_{m-N}, \sin\vartheta_{m-N})}{|\boldsymbol{x}_m - \boldsymbol{\xi}_k|^2}$$

$$+\gamma\sum_{k=N+1}^{2N} c_k\frac{(\boldsymbol{x}_m-\boldsymbol{\xi}_k)\cdot(\cos\vartheta_{m-N},\sin\vartheta_{m-N})}{|\boldsymbol{x}_m-\boldsymbol{\xi}_k|^2}+\gamma\sum_{k=2N+1}^{3N} c_k\frac{(\boldsymbol{x}_m-\boldsymbol{\xi}_k)\cdot(\cos\vartheta_{m-N},\sin\vartheta_{m-N})}{|\boldsymbol{x}_m-\boldsymbol{\xi}_k|^2},$$

$m=\overline{N+1,2N}$,

$$J_{j,5N+1}=\sum_{k=1}^{3N} c_k\,\frac{\partial G(\boldsymbol{\xi}_k,\boldsymbol{x}_j)}{\partial\eta^a_{\rm int}}=-\gamma\sum_{k=1}^{N} c_k r_k\frac{(\boldsymbol{x}_j-\boldsymbol{\xi}_k)\cdot(\cos\vartheta_k,\sin\vartheta_k)}{|\boldsymbol{x}_j-\boldsymbol{\xi}_k|^2},\quad j=\overline{N+1,2N},$$

$$J_{j,5N+2}=\sum_{k=1}^{3N} c_k\,\frac{\partial G(\boldsymbol{\xi}_k,\boldsymbol{x}_j)}{\partial\eta^b_{\rm int}}=-\gamma\sum_{k=N+1}^{2N} c_k r_k\frac{(\boldsymbol{x}_j-\boldsymbol{\xi}_k)\cdot(\cos\vartheta_{k-N},\sin\vartheta_{k-N})}{|\boldsymbol{x}_j-\boldsymbol{\xi}_k|^2},\quad j=\overline{N+1,2N},$$

$$J_{j,5N+3}=\sum_{k=1}^{3N} c_k\,\frac{\partial G(\boldsymbol{\xi}_k,\boldsymbol{x}_j)}{\partial\eta_{\rm ext}}=-\gamma\sum_{k=2N+1}^{3N} c_k R\frac{(\boldsymbol{x}_j-\boldsymbol{\xi}_k)\cdot(\cos\vartheta_{k-2N},\sin\vartheta_{k-2N})}{|\boldsymbol{x}_j-\boldsymbol{\xi}_k|^2},\quad j=\overline{N+1,2N},$$

$$J_{j,5N+4}=\sum_{k=1}^{2N} c_k\,\frac{\partial G(\boldsymbol{\xi}_k,\boldsymbol{x}_j)}{\partial X^a}=-\gamma\sum_{k=1}^{N} c_k\frac{(\boldsymbol{x}_j-\boldsymbol{\xi}_k)_x}{|\boldsymbol{x}_j-\boldsymbol{\xi}_k|^2},\quad j=\overline{N+1,2N},$$

$$J_{j,5N+5}=-\gamma\sum_{k=1}^{N} c_k\frac{(\boldsymbol{x}_j-\boldsymbol{\xi}_k)_y}{|\boldsymbol{x}_j-\boldsymbol{\xi}_k|^2},\quad j=\overline{N+1,2N},$$

$$J_{j,5N+6}=\sum_{k=1}^{2N} c_k\,\frac{\partial G(\boldsymbol{\xi}_k,\boldsymbol{x}_j)}{\partial X^b}=\gamma\sum_{k=1}^{N} c_k\frac{(\boldsymbol{x}_j-\boldsymbol{\xi}_k)_x}{|\boldsymbol{x}_j-\boldsymbol{\xi}_k|^2}+\gamma\sum_{k=2N+1}^{3N} c_k\frac{(\boldsymbol{x}_j-\boldsymbol{\xi}_k)_x}{|\boldsymbol{x}_j-\boldsymbol{\xi}_k|^2},\quad j=\overline{N+1,2N},$$

$$J_{j,5N+7}=\sum_{k=1}^{2N} c_k\,\frac{\partial G(\boldsymbol{\xi}_k,\boldsymbol{x}_j)}{\partial Y^b}=\gamma\sum_{k=1}^{N} c_k\frac{(\boldsymbol{x}_j-\boldsymbol{\xi}_k)_y}{|\boldsymbol{x}_j-\boldsymbol{\xi}_k|^2}+\gamma\sum_{k=2N+1}^{3N} c_k\frac{(\boldsymbol{x}_j-\boldsymbol{\xi}_k)_y}{|\boldsymbol{x}_j-\boldsymbol{\xi}_k|^2},\quad j=\overline{N+1,2N},$$

$$F_j=\sum_{k=1}^{3N} c_k\,G(\boldsymbol{\xi}_k,\boldsymbol{x}_j)-f(\boldsymbol{x}_j)$$

$$=\gamma\sum_{k=1}^{N} c_k\log\sqrt{\Big(R\cos\tilde\vartheta_{j-2N}-X^a-\eta^a_{\rm int}r_k\cos\vartheta_k\Big)^2+\Big(R\sin\tilde\vartheta_{j-2N}-Y^a-\eta^a_{\rm int}r_k\sin\vartheta_k\Big)^2}$$

$$+\gamma\sum_{k=N+1}^{2N} c_k\log\sqrt{\Big(R\cos\tilde\vartheta_{j-2N}-X^b-\eta^b_{\rm int}r_k\cos\vartheta_k\Big)^2+\Big(R\sin\tilde\vartheta_{j-2N}-Y^b-\eta^b_{\rm int}r_k\sin\vartheta_k\Big)^2}$$

$$+\gamma\sum_{k=2N+1}^{3N} c_k\log\sqrt{\Big(R\cos\tilde\vartheta_{j-2N}-\eta_{\rm ext}R\cos\vartheta_{k-2N}\Big)^2+\Big(R\sin\tilde\vartheta_{j-2N}-\eta_{\rm ext}R\sin\vartheta_{k-2N}\Big)^2}-f(\boldsymbol{x}_j),$$

$j=\overline{2N+1,2N+M}$,

. . . . . .

$$J_{j,m}=G(\boldsymbol{\xi}_m,\boldsymbol{x}_j),\quad j=\overline{2N+1,2N+M},\ m=\overline{1,3N},$$

$$J_{j,3N+m} = \frac{\partial}{\partial r_m} \sum_{k=1}^{3N} c_k \, G(\boldsymbol{\xi}_k, \boldsymbol{x}_j)$$

$$= -\gamma \eta_{\text{int}}^a c_m \frac{(\boldsymbol{x}_j - \boldsymbol{\xi}_m) \cdot (\cos\vartheta_m, \sin\vartheta_m)}{|\boldsymbol{x}_j - \boldsymbol{\xi}_m|^2}, \quad j = \overline{2N+1, 2N+M}, \ m = \overline{1, N},$$

$$J_{j,3N+m} = \frac{\partial}{\partial r_m} \sum_{k=1}^{2N} c_k \, G(\boldsymbol{\xi}_k, \boldsymbol{x}_j) = -\gamma \eta_{\text{int}}^b c_m \frac{(\boldsymbol{x}_j - \boldsymbol{\xi}_m) \cdot (\cos\vartheta_{m-N}, \sin\vartheta_{m-N})}{|\boldsymbol{x}_j - \boldsymbol{\xi}_m|^2},$$

$$j = \overline{2N+1, 2N+M}, \ m = \overline{N+1, 2N},$$

$$J_{j,5N+1} = \sum_{k=1}^{3N} c_k \frac{\partial G(\boldsymbol{\xi}_k, \boldsymbol{x}_j)}{\partial \eta_{\text{int}}^a} = -\gamma \sum_{k=1}^{N} c_k r_k \frac{(\boldsymbol{x}_j - \boldsymbol{\xi}_k) \cdot (\cos\vartheta_k, \sin\vartheta_k)}{|\boldsymbol{x}_j - \boldsymbol{\xi}_k|^2}, \quad j = \overline{2N+1, 2N+M},$$

$$J_{j,5N+2} = \sum_{k=1}^{3N} c_k \frac{\partial G(\boldsymbol{\xi}_k, \boldsymbol{x}_j)}{\partial \eta_{\text{int}}^b} = -\gamma \sum_{k=N+1}^{2N} c_k r_k \frac{(\boldsymbol{x}_j - \boldsymbol{\xi}_k) \cdot (\cos\vartheta_{k-N}, \sin\vartheta_{k-N})}{|\boldsymbol{x}_j - \boldsymbol{\xi}_k|^2},$$

$$j = \overline{2N+1, 2N+M},$$

$$J_{j,5N+3} = \sum_{k=1}^{3N} c_k \frac{\partial G(\boldsymbol{\xi}_k, \boldsymbol{x}_j)}{\partial \eta_{\text{ext}}} = -\gamma \sum_{k=2N+1}^{3N} c_k R \frac{(\boldsymbol{x}_j - \boldsymbol{\xi}_k) \cdot (\cos\vartheta_{k-2N}, \sin\vartheta_{k-2N})}{|\boldsymbol{x}_j - \boldsymbol{\xi}_k|^2},$$

$$j = \overline{2N+1, 2N+M},$$

$$J_{j,5N+4} = \sum_{k=1}^{3N} c_k \frac{\partial G(\boldsymbol{\xi}_k, \boldsymbol{x}_j)}{\partial X^a} = -\gamma \sum_{k=1}^{N} c_k \frac{(\boldsymbol{x}_j - \boldsymbol{\xi}_k)_x}{|\boldsymbol{x}_j - \boldsymbol{\xi}_k|^2}, \quad j = \overline{2N+1, 2N+M},$$

$$J_{j,5N+5} = \sum_{k=1}^{3N} c_k \frac{\partial G(\boldsymbol{\xi}_k, \boldsymbol{x}_j)}{\partial Y^a} = -\gamma \sum_{k=1}^{N} c_k \frac{(\boldsymbol{x}_j - \boldsymbol{\xi}_k)_y}{|\boldsymbol{x}_j - \boldsymbol{\xi}_k|^2}, \quad j = \overline{2N+1, 2N+M},$$

$$J_{j,5N+6} = \sum_{k=1}^{3N} c_k \frac{\partial G(\boldsymbol{\xi}_k, \boldsymbol{x}_j)}{\partial X^b} = -\gamma \sum_{k=N+1}^{2N} c_k \frac{(\boldsymbol{x}_j - \boldsymbol{\xi}_k)_x}{|\boldsymbol{x}_j - \boldsymbol{\xi}_k|^2}, \quad j = \overline{2N+1, 2N+M},$$

$$J_{j,5N+6} = \sum_{k=1}^{3N} c_k \frac{\partial G(\boldsymbol{\xi}_k, \boldsymbol{x}_j)}{\partial Y^b} = -\gamma \sum_{k=N+1}^{2N} c_k \frac{(\boldsymbol{x}_j - \boldsymbol{\xi}_k)_y}{|\boldsymbol{x}_j - \boldsymbol{\xi}_k|^2}, \quad j = \overline{2N+1, 2N+M},$$

$$F_{M+j} = \sum_{k=1}^{3N} c_k \, \partial_n G(\boldsymbol{\xi}_k, \boldsymbol{x}_j) - g^{\varepsilon}(\boldsymbol{x}_j) = \gamma \sum_{k=1}^{3N} c_k \frac{(\boldsymbol{x}_j - \boldsymbol{\xi}_k) \cdot \boldsymbol{n}_j}{|\boldsymbol{x}_j - \boldsymbol{\xi}_k|^2} - g^{\varepsilon}(\boldsymbol{x}_j)$$

$$= \gamma \sum_{k=1}^{N} c_k \frac{\left(R\cos\tilde{\vartheta}_{j-2N} - X^a - \eta_{\text{int}}^a r_k \cos\vartheta_k\right)\cos\tilde{\vartheta}_{j-2N} + \left(R\sin\tilde{\vartheta}_{j-2N} - Y^a - \eta_{\text{int}}^a r_k \sin\vartheta_k\right)\sin\tilde{\vartheta}_{j-2N}}{\left(R\cos\tilde{\vartheta}_{j-2N} - X^a - \eta_{\text{int}}^a r_k \cos\vartheta_k\right)^2 + \left(R\sin\tilde{\vartheta}_{j-2N} - Y^a - \eta_{\text{int}}^a r_k \sin\vartheta_k\right)^2}$$

$$+\gamma\sum_{k=N+1}^{2N} c_k \frac{\left(R\cos\tilde{\vartheta}_{j-2N}-X^b-\eta_{\rm int}^b r_k\cos\vartheta_k\right)\cos\tilde{\vartheta}_{j-2N}+\left(R\sin\tilde{\vartheta}_{j-2N}-Y^b-\eta_{\rm int}^b r_k\sin\vartheta_k\right)\sin\tilde{\vartheta}_{j-2N}}{\left(R\cos\tilde{\vartheta}_{j-2N}-X^b-\eta_{\rm int}^b r_k\cos\vartheta_k\right)^2+\left(R\sin\tilde{\vartheta}_{j-2N}-Y^b-\eta_{\rm int}^b r_k\sin\vartheta_k\right)^2}$$

$$+\gamma\sum_{k=2N+1}^{3N} c_k \frac{\left(R\cos\tilde{\vartheta}_{j-2N}-\eta_{\rm ext}R\cos\vartheta_{k-2N}\right)\cos\tilde{\vartheta}_{j-2N}+\left(R\sin\tilde{\vartheta}_{j-2N}-\eta_{\rm ext}R\sin\vartheta_{k-2N}\right)\sin\tilde{\vartheta}_{j-2N}}{\left(R\cos\tilde{\vartheta}_{j-2N}-\eta_{\rm ext}R\cos\vartheta_{k-2N}\right)^2+\left(R\sin\tilde{\vartheta}_{j-2N}-\eta_{\rm ext}R\sin\vartheta_{k-2N}\right)^2}$$

$$-g^{\varepsilon}(\boldsymbol{x}_j),\quad j=\overline{2N+1,2N+M},$$

. . . . . .

$$J_{M+j,m}=\partial_n G(\boldsymbol{\xi}_m,\boldsymbol{x}_j)=\gamma\frac{(\boldsymbol{x}_j-\boldsymbol{\xi}_m)\cdot\boldsymbol{n}_j}{|\boldsymbol{x}_j-\boldsymbol{\xi}_m|^2},\quad j=\overline{2N+1,2N+M},\ m=\overline{1,3N},$$

$$J_{M+j,3N+m}=\frac{\partial}{\partial r_m}\sum_{k=1}^{3N} c_k\,\partial_n G(\boldsymbol{\xi}_k,\boldsymbol{x}_j)$$

$$=\gamma\eta_{\rm int}^a c_m\Bigg[-\frac{(\cos\vartheta_m\cos\tilde{\vartheta}_{j-2N}+\sin\vartheta_m\sin\tilde{\vartheta}_{j-2N})}{|\boldsymbol{x}_j-\boldsymbol{\xi}_m|^2}$$

$$+2\frac{(\boldsymbol{x}_j-\boldsymbol{\xi}_m)\cdot\boldsymbol{n}_j}{|\boldsymbol{x}_j-\boldsymbol{\xi}_m|^4}\left((\boldsymbol{x}_j-\boldsymbol{\xi}_m)\cdot(\cos\vartheta_m,\sin\vartheta_m)\right)\Bigg],$$

$$j=\overline{2N+1,2N+M},\ m=\overline{1,N},$$

$$J_{M+j,3N+m}=\frac{\partial}{\partial r_m}\sum_{k=1}^{3N} c_k\,\partial_n G(\boldsymbol{\xi}_k,\boldsymbol{x}_j)$$

$$=\gamma\eta_{\rm int}^b c_m\Bigg[-\frac{(\cos\vartheta_{m-N}\cos\tilde{\vartheta}_{j-2N}+\sin\vartheta_{m-N}\sin\tilde{\vartheta}_{j-2N})}{|\boldsymbol{x}_j-\boldsymbol{\xi}_m|^2}$$

$$+2\frac{(\boldsymbol{x}_j-\boldsymbol{\xi}_m)\cdot\boldsymbol{n}_j}{|\boldsymbol{x}_j-\boldsymbol{\xi}_m|^4}\left((\boldsymbol{x}_j-\boldsymbol{\xi}_m)\cdot(\cos\vartheta_{m-N},\sin\vartheta_{m-N})\right)\Bigg],$$

$$j=\overline{2N+1,2N+M},\ m=\overline{N+1,2N},$$

$$J_{M+j,5N+1}=\sum_{k=1}^{3N} c_k\,\frac{\partial\left(\partial_n G(\boldsymbol{\xi}_k,\boldsymbol{x}_j)\right)}{\partial\eta_{\rm int}^a}$$

$$=\gamma\sum_{k=1}^{N} c_k r_k\Bigg[-\frac{(\cos\vartheta_k\cos\tilde{\vartheta}_{j-2N}+\sin\vartheta_k\sin\tilde{\vartheta}_{j-2N})}{|\boldsymbol{x}_j-\boldsymbol{\xi}_k|^2}$$

$$+2\frac{(\boldsymbol{x}_j-\boldsymbol{\xi}_k)\cdot\boldsymbol{n}_j}{|\boldsymbol{x}_j-\boldsymbol{\xi}_k|^4}\left((\boldsymbol{x}_j-\boldsymbol{\xi}_k)\cdot(\cos\vartheta_k,\sin\vartheta_k)\right)\Bigg],\quad j=\overline{2N+1,2N+M},$$

$$J_{M+j,5N+2} = \sum_{k=1}^{2N} c_k \frac{\partial\left(\partial_n G(\boldsymbol{\xi}_k, \boldsymbol{x}_j)\right)}{\partial \eta_{\text{int}}^b}$$

$$= \gamma \sum_{k=N+1}^{2N} c_k r_k \Bigg[- \frac{(\cos\vartheta_{k-N}\cos\tilde{\vartheta}_{j-2N} + \sin\vartheta_{k-N}\sin\tilde{\vartheta}_{j-2N})}{|\boldsymbol{x}_j - \boldsymbol{\xi}_k|^2}$$

$$+2\frac{(\boldsymbol{x}_j - \boldsymbol{\xi}_k)\cdot \boldsymbol{n}_j}{|\boldsymbol{x}_j - \boldsymbol{\xi}_k|^4}\left((\boldsymbol{x}_j - \boldsymbol{\xi}_k)\cdot(\cos\vartheta_k, \sin\vartheta_k)\right)\Bigg], \quad j = \overline{2N+1, 2N+M},$$

$$J_{M+j,5N+3} = \sum_{k=1}^{3N} c_k \frac{\partial\left(\partial_n G(\boldsymbol{\xi}_k, \boldsymbol{x}_j)\right)}{\partial \eta_{\text{ext}}} = \gamma \sum_{k=2N+1}^{3N} c_k R \left[- \frac{(\cos\vartheta_{k-2N}\cos\tilde{\vartheta}_{j-2N} + \sin\vartheta_{k-2N}\sin\tilde{\vartheta}_{j-2N})}{|\boldsymbol{x}_j - \boldsymbol{\xi}_k|^2}\right.$$

$$\left. +2\frac{(\boldsymbol{x}_j - \boldsymbol{\xi}_k)\cdot \boldsymbol{n}_j}{|\boldsymbol{x}_j - \boldsymbol{\xi}_k|^4}\left((\boldsymbol{x}_j - \boldsymbol{\xi}_k)\cdot(\cos\vartheta_{k-2N}, \sin\vartheta_{k-2N})\right)\right], \ j = \overline{2N+1, 2N+M},$$

$$J_{M+j,5N+4} = \sum_{k=1}^{3N} c_k \frac{\partial\left(\partial_n G(\boldsymbol{\xi}_k, \boldsymbol{x}_j)\right)}{\partial X^a}$$

$$= \gamma \sum_{k=1}^{N} c_k \left[- \frac{\cos\tilde{\vartheta}_{j-2N}}{|\boldsymbol{x}_j - \boldsymbol{\xi}_k|^2} + 2\frac{(\boldsymbol{x}_j - \boldsymbol{\xi}_k)\cdot \boldsymbol{n}_j}{|\boldsymbol{x}_j - \boldsymbol{\xi}_k|^4}\left(\boldsymbol{x}_j - \boldsymbol{\xi}_k\right)_x\right], \ j = \overline{2N+1, 2N+M},$$

$$J_{M+j,5N+5} = \sum_{k=1}^{3N} c_k \frac{\partial\left(\partial_n G(\boldsymbol{\xi}_k, \boldsymbol{x}_j)\right)}{\partial Y^a}$$

$$= \gamma \sum_{k=1}^{N} c_k \left[- \frac{\sin\tilde{\vartheta}_{j-2N}}{|\boldsymbol{x}_j - \boldsymbol{\xi}_k|^2} + 2\frac{(\boldsymbol{x}_j - \boldsymbol{\xi}_k)\cdot \boldsymbol{n}_j}{|\boldsymbol{x}_j - \boldsymbol{\xi}_k|^4}\left(\boldsymbol{x}_j - \boldsymbol{\xi}_k\right)_y\right], \ j = \overline{2N+1, 2N+M},$$

$$J_{M+j,5N+6} = \sum_{k=1}^{3N} c_k \frac{\partial\left(\partial_n G(\boldsymbol{\xi}_k, \boldsymbol{x}_j)\right)}{\partial X^b}$$

$$= \gamma \sum_{k=N+1}^{2N} c_k \left[- \frac{\cos\tilde{\vartheta}_{j-2N}}{|\boldsymbol{x}_j - \boldsymbol{\xi}_k|^2} + 2\frac{(\boldsymbol{x}_j - \boldsymbol{\xi}_k)\cdot \boldsymbol{n}_j}{|\boldsymbol{x}_j - \boldsymbol{\xi}_k|^4}\left(\boldsymbol{x}_j - \boldsymbol{\xi}_k\right)_x\right], \ j = \overline{2N+1, 2N+M},$$

$$J_{M+j,5N+7} = \sum_{k=1}^{3N} c_k \frac{\partial\left(\partial_n G(\boldsymbol{\xi}_k, \boldsymbol{x}_j)\right)}{\partial Y^a}$$

$$= \gamma \sum_{k=N+1}^{2N} c_k \left[- \frac{\sin\tilde{\vartheta}_{j-2N}}{|\boldsymbol{x}_j - \boldsymbol{\xi}_k|^2} + 2\frac{(\boldsymbol{x}_j - \boldsymbol{\xi}_k)\cdot \boldsymbol{n}_j}{|\boldsymbol{x}_j - \boldsymbol{\xi}_k|^4}\left(\boldsymbol{x}_j - \boldsymbol{\xi}_k\right)_y\right], \ j = \overline{2N+1, 2N+M},$$

$$F_{2M+2N+1} = \sqrt{\lambda_1 \sum_{\ell=1}^{3N} c_\ell^2},$$

$$J_{2M+2N+1,m} = \frac{\partial}{\partial c_m}\sqrt{\lambda_1 \sum_{\ell=1}^{3N} c_\ell^2} = \sqrt{\lambda_1}\,\frac{c_m}{\sqrt{\sum_{\ell=1}^{3N} c_\ell^2}}, \quad m = \overline{1,3N},$$

$$J_{2M+2N+1,3N+m} = \frac{\partial}{\partial r_m}\sqrt{\lambda_1 \sum_{\ell=1}^{3N} c_\ell^2} = 0,\ m = \overline{1,2N},$$

$$J_{2M+2N+1,5N+1} = \frac{\partial}{\partial \eta_{\text{int}}^a}\sqrt{\lambda_1 \sum_{\ell=1}^{3N} c_\ell^2} = 0,$$

$$J_{2M+2N+1,5N+2} = \frac{\partial}{\partial \eta_{\text{int}}^b}\sqrt{\lambda_1 \sum_{\ell=1}^{3N} c_\ell^2} = 0,$$

$$J_{2M+2N+1,5N+3} = \frac{\partial}{\partial \eta_{\text{ext}}}\sqrt{\lambda_1 \sum_{\ell=1}^{3N} c_\ell^2} = 0,$$

$$J_{2M+2N+1,5N+4} = \frac{\partial}{\partial X^a}\sqrt{\lambda_1 \sum_{\ell=1}^{3N} c_\ell^2} = 0,$$

$$J_{2M+2N+1,5N+5} = \frac{\partial}{\partial Y^a}\sqrt{\lambda_1 \sum_{\ell=1}^{3N} c_\ell^2} = 0,$$

$$J_{2M+2N+1,5N+6} = \frac{\partial}{\partial X^b}\sqrt{\lambda_1 \sum_{\ell=1}^{3N} c_\ell^2} = 0,$$

$$J_{2M+2N+1,5N+7} = \frac{\partial}{\partial Y^b}\sqrt{\lambda_1 \sum_{\ell=1}^{3N} c_\ell^2} = 0,$$

$$F_{2M+2N+2} = \sqrt{\lambda_2 \sum_{\ell=2}^{N} (r_\ell - r_{\ell-1})^2},$$

$$J_{2M+2N+2,m} = \frac{\partial}{\partial c_m}\sqrt{\lambda_2 \sum_{\ell=2}^{N} (r_\ell - r_{\ell-1})^2} = 0,\ m = \overline{1,3N},$$

$$J_{2M+2N+2,3N+1}=\frac{\partial}{\partial r_1}\sqrt{\lambda_2\sum_{\ell=2}^{N}\left(r_\ell-r_{\ell-1}\right)^2}=-\sqrt{\lambda_2}\,\frac{(r_2-r_1)}{\sqrt{\sum_{\ell=2}^{N}\left(r_\ell-r_{\ell-1}\right)^2}},$$

$$J_{2M+2N+2,3N+m}=\frac{\partial}{\partial r_m}\sqrt{\lambda_2\sum_{\ell=2}^{N}\left(r_\ell-r_{\ell-1}\right)^2}=\sqrt{\lambda_2}\,\frac{(2r_m-r_{m-1}-r_{m+1})}{\sqrt{\sum_{\ell=2}^{N}\left(r_\ell-r_{\ell-1}\right)^2}},\ m=\overline{2,N-1},$$

$$J_{2M+2N+2,3N+N}=\frac{\partial}{\partial r_N}\sqrt{\lambda_2\sum_{\ell=2}^{N}\left(r_\ell-r_{\ell-1}\right)^2}=\sqrt{\lambda_2}\,\frac{(r_N-r_{N-1})}{\sqrt{\sum_{\ell=2}^{N}\left(r_\ell-r_{\ell-1}\right)^2}},$$

$$J_{2M+2N+2,3N+m}=\frac{\partial}{\partial r_m}\sqrt{\lambda_2\sum_{\ell=2}^{N}\left(r_\ell-r_{\ell-1}\right)^2}=0,\ m=\overline{N+1,2N},$$

$$J_{2M+2N+2,5N+1}=\frac{\partial}{\partial \eta^a_{\text{int}}}\sqrt{\lambda_2\sum_{\ell=2}^{N}\left(r_\ell-r_{\ell-1}\right)^2}=0,$$

$$J_{2M+2N+2,5N+2}=\frac{\partial}{\partial \eta^b_{\text{int}}}\sqrt{\lambda_2\sum_{\ell=2}^{N}\left(r_\ell-r_{\ell-1}\right)^2}=0,$$

$$J_{2M+2N+2,5N+3}=\frac{\partial}{\partial \eta_{\text{ext}}}\sqrt{\lambda_2\sum_{\ell=2}^{N}\left(r_\ell-r_{\ell-1}\right)^2}=0,$$

$$J_{2M+2N+2,5N+4}=\frac{\partial}{\partial X^a}\sqrt{\lambda_2\sum_{\ell=2}^{N}\left(r_\ell-r_{\ell-1}\right)^2}=0,$$

$$J_{2M+2N+2,5N+5}=\frac{\partial}{\partial Y^a}\sqrt{\lambda_2\sum_{\ell=2}^{N}\left(r_\ell-r_{\ell-1}\right)^2}=0.$$

$$J_{2M+2N+2,5N+6}=\frac{\partial}{\partial X^b}\sqrt{\lambda_2\sum_{\ell=2}^{N}\left(r_\ell-r_{\ell-1}\right)^2}=0,$$

$$J_{2M+2N+2,5N+7}=\frac{\partial}{\partial Y^b}\sqrt{\lambda_2\sum_{\ell=2}^{N}\left(r_\ell-r_{\ell-1}\right)^2}=0.$$

$$F_{2M+2N+3}=\sqrt{\lambda_3\sum_{\ell=2}^{N}\left(r_{N+\ell}-r_{N+\ell-1}\right)^2},$$

$$J_{2M+2N+3,m} = \frac{\partial}{\partial c_m}\sqrt{\lambda_3 \sum_{\ell=2}^{N} \left(r_\ell - r_{\ell-1}\right)^2} = 0,\ m = \overline{1,3N},$$

$$J_{2M+2N+3,3N+m} = \frac{\partial}{\partial r_m}\sqrt{\lambda_3 \sum_{\ell=2}^{N} \left(r_{N+\ell} - r_{N+\ell-1}\right)^2} = 0,\ m = \overline{1,N},$$

$$J_{2M+2N+3,4N+1} = \frac{\partial}{\partial r_{N+1}}\sqrt{\lambda_3 \sum_{\ell=2}^{N} \left(r_{N+\ell} - r_{N+\ell-1}\right)^2} = -\sqrt{\lambda_3}\,\frac{\left(r_{N+2} - r_{N+1}\right)}{\sqrt{\sum_{\ell=2}^{N} \left(r_{N+\ell} - r_{N+\ell-1}\right)^2}},$$

$$J_{2M+2N+3,3N+m} = \frac{\partial}{\partial r_m}\sqrt{\lambda_3 \sum_{\ell=2}^{N} \left(r_{N+\ell} - r_{N+\ell-1}\right)^2} = \sqrt{\lambda_3}\,\frac{\left(2r_m - r_{m-1} - r_{m+1}\right)}{\sqrt{\sum_{\ell=2}^{N} \left(r_{N+\ell} - r_{N+\ell-1}\right)^2}},$$

$m = \overline{N+2, 2N-1}$,

$$J_{2M+2N+3,5N} = \frac{\partial}{\partial r_{2N}}\sqrt{\lambda_3 \sum_{\ell=2}^{N} \left(r_{N+\ell} - r_{N+\ell-1}\right)^2} = \sqrt{\lambda_3}\,\frac{\left(r_{2N} - r_{2N-1}\right)}{\sqrt{\sum_{\ell=2}^{N} \left(r_{N+\ell} - r_{N+\ell-1}\right)^2}},$$

$$J_{2M+2N+3,3N+m} = \frac{\partial}{\partial r_m}\sqrt{\lambda_3 \sum_{\ell=2}^{N} \left(r_{N+\ell} - r_{N+\ell-1}\right)^2} = 0,\ m = \overline{N+1, 2N},$$

$$J_{2M+2N+3,5N+1} = \frac{\partial}{\partial \eta^a_{\text{int}}}\sqrt{\lambda_3 \sum_{\ell=2}^{N} \left(r_{N+\ell} - r_{N+\ell-1}\right)^2} = 0,$$

$$J_{2M+2N+3,5N+2} = \frac{\partial}{\partial \eta^b_{\text{int}}}\sqrt{\lambda_3 \sum_{\ell=2}^{N} \left(r_{N+\ell} - r_{N+\ell-1}\right)^2} = 0,$$

$$J_{2M+2N+3,5N+3} = \frac{\partial}{\partial \eta_{\text{ext}}}\sqrt{\lambda_3 \sum_{\ell=2}^{N} \left(r_{N+\ell} - r_{N+\ell-1}\right)^2} = 0,$$

$$J_{2M+2N+3,5N+4} = \frac{\partial}{\partial X^a}\sqrt{\lambda_3 \sum_{\ell=2}^{N} \left(r_{N+\ell} - r_{N+\ell-1}\right)^2} = 0,$$

$$J_{2M+2N+3,5N+5} = \frac{\partial}{\partial Y^a}\sqrt{\lambda_3 \sum_{\ell=2}^{N} \left(r_{N+\ell} - r_{N+\ell-1}\right)^2} = 0.$$

TABLE 2. Example 5: CPU times in seconds with number of iterations, with and without providing the Jacobian, no noise and no regularization.

`niter`	With Jacobian	Without Jacobian
10	0.1357	1.4740
20	0.3502	2.4180
50	0.5445	5.7470
100	1.2196	11.218
500	4.2579	58.854
1000	8.0454	153.13
2000	13.887	416.57
5000	37.127	1828.7

$$J_{2M+2N+3,5N+6} = \frac{\partial}{\partial X^b}\sqrt{\lambda_3 \sum_{\ell=2}^{N} \left(r_{N+\ell} - r_{N+\ell-1}\right)^2} = 0,$$

$$J_{2M+2N+3,5N+7} = \frac{\partial}{\partial Y^b}\sqrt{\lambda_3 \sum_{\ell=2}^{N} \left(r_{N+\ell} - r_{N+\ell-1}\right)^2} = 0.$$

6.2. **Example 5.** We consider the case of a multiple void made up a bean–shaped obstacle Ω_1^a and a peanut–shaped obstacle Ω_1^b are present. The obstacle Ω_1^a is described by the radial parametrization

$$r^a(\vartheta) = 0.5\,\left(\frac{0.5 + 0.4\cos(\vartheta) + 0.1\sin(2\vartheta)}{1 + 0.7\cos(\vartheta)}\right), \quad \vartheta \in [0, 2\pi), \tag{6.8}$$

while Ω_1^b is described by

$$r(\vartheta) = 0.3\sqrt{\cos^2(\vartheta) + 0.25\sin^2(\vartheta)}\,, \quad \vartheta \in [0, 2\pi), \tag{6.9}$$

and have centres $X^a = -0.3, Y^a = 0.3$ and $X^b = 0.3, Y^b = -0.3$, respectively. In this example, we consider the homogeneous Dirichlet boundary conditions with $\alpha_1 = \alpha_2 = 1$ on the boundaries of both rigid inclusions. The Neumann data (6.1c) is simulated by solving the direct boundary value problem (6.1) (without (6.1c) and with f in (6.1b) given by (5.1)) using the MFS with $M = N = 400$. In order to avoid committing an inverse crime, the inverse solver is applied using $N = 40, M = 125$. Moreover, we took the initial vector of unknowns $\mathbf{x}^0 = \left(\boldsymbol{c}_0, \boldsymbol{r}_0^a, \boldsymbol{r}_0^b, , \eta_{\text{int}}^{a^0}, \eta_{\text{int}}^{b^0}, \eta_{\text{ext}}^0, X_0^a, Y_0^a, X_0^b, Y_0^b\right) = (\mathbf{0}, \mathbf{0.1}, \mathbf{0.1}, 0.5, 0.5, 1.5, -0.5, 0.2, 0.5, -0.2)$.

In Table 2 we present the CPU times required for the above parameters for different numbers of iterations when providing and when not providing the Jacobian. The savings when providing the Jacobian are spectacular.

In Figure 15 we present the reduction of the residual after 500 iterations, no noise and no regularization, when providing the Jacobian and when not providing the Jacobian. As can be observed, when providing the Jacobian the residual functional (6.7) decreases faster than when the Jacobian is not provided.

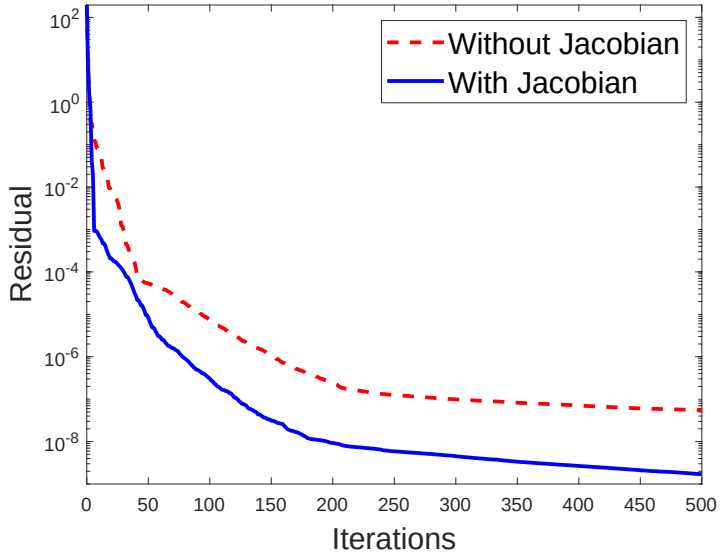

FIGURE 15. Example 5: Residual functional (6.7) with the number of iterations.

In Figure 16 we present the results obtained for different numbers of iterations and no regularization. In Figures 17 and 18 we present the corresponding reconstructed curves with a noise level of $p = 5\%$, after 1000 iterations, and various levels of regularization λ_1 with $\lambda_2 = \lambda_2^a = \lambda_2^b = 0$, and $\lambda_1 = 0$ with $\lambda_2 = \lambda_2^a = \lambda_2^b$, respectively. Overall, Figures 16–18 illustrate that the MFS can indeed retrieve successfully voids having two connected components.

7. Conclusions

In this study, we have investigated the performance of the MFS for the solution of inverse geometric problems governed by the Laplace equation. In particular, we have considered the problem of determining a rigid inclusion or a cavity. The MFS discretization led to a nonlinear system of equations for the coefficients in the MFS expansion, the radial radii, the contraction and dilation coefficients and the coordinates of the centre of the cavity. For the solution of the nonlinear system we have used the MATLAB® optimization toolbox routine `lsqnonlin`. In previous studies, such as [16], we had chosen the option of not providing the Jacobian of the system which was calculated internally. In the current work we do provide the Jacobian of the system and show that this leads to considerable savings in computational time, rapid convergence as well as accurate reconstructions of the unknown void. The method is extended to the case of two voids. In future studies we plan to investigate the corresponding application to three–dimensional problems.

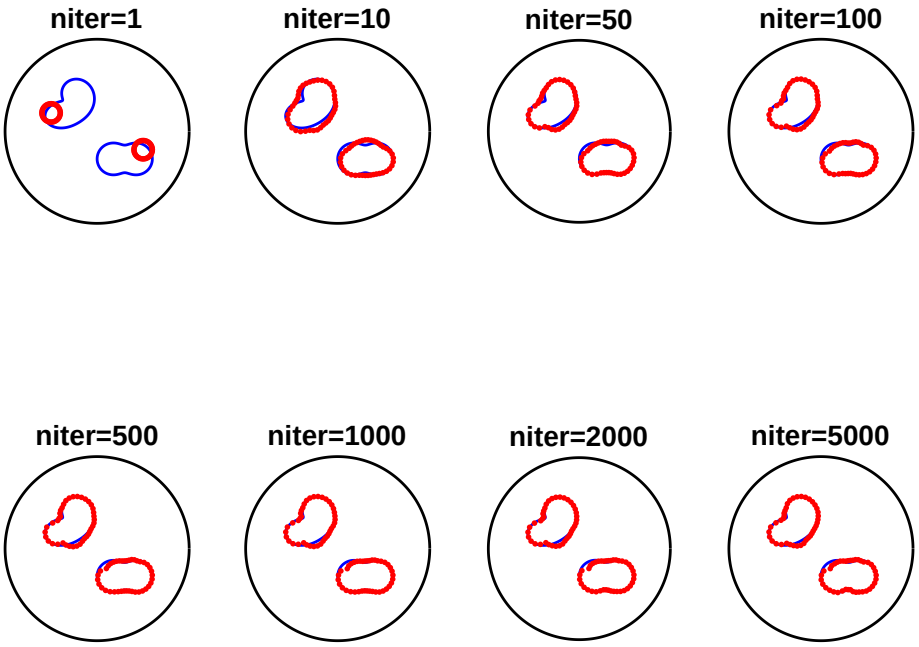

FIGURE 16. Example 5: Results for various numbers of iterations for no noise and no regularization.

REFERENCES

[1] G. Alessandrini and L. Rondi, *Optimal stability for the inverse problem of multiple cavities*, J. Diff. Equations **176** (2001), 356–386.

[2] M. Belge, M. E. Kilmer, E. L. Miller, *Efficient determination of multiple regularization parameters in a generalized L-curve framework*, Inverse Probl. **18** (2002) 1161–1183.

[3] J.R. Berger and A. Karageorghis, *The method of fundamental solutions for heat conduction in layered materials*, Int. J. Numer. Methods Eng. **45** (1999), 1681–1694.

[4] B. Bin-Mohsin and D. Lesnic, *Reconstruction of a source domain from boundary measurements*, Appl. Math. Model. **45** (2017), 925–939.

[5] Z. Chen, Y. Lu, Y. Xu, H. Yang, *Multi-parameter Tikhonov regularization for linear ill-posed operator equations*, J. Comput. Math. **26** (2008) 37–55.

[6] T. F. Coleman and Y. Li, *On the convergence of interior-reflective Newton methods for nonlinear minimization subject to bounds*, Math. Programming **67** (1994), 189–224.

[7] T. F. Coleman and Y. Li, *An interior trust region approach for nonlinear minimization subject to bounds*, SIAM J. Optim. **6** (1996), 418–445.

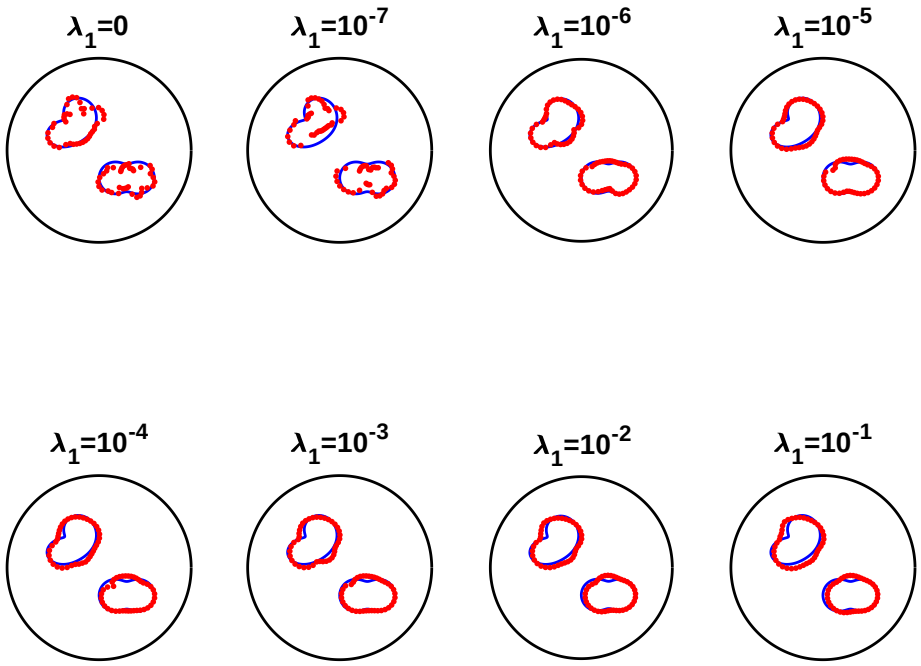

FIGURE 17. Example 5: Results for noise $p = 5\%$ and regularization with λ_1.

[8] G. Fairweather and A. Karageorghis, *The method of fundamental solution for elliptic boundary value problems*, Adv. Comput. Math. **9** (1998), 69–95.
[9] P. Gorzelańczyk and J. A. Kołodziej, *Some remarks concerning the shape of the source contour with application of the method of fundamental solutions to elastic torsion of prismatic rods*, Eng. Anal. Bound. Elem. **37** (2008), 64–75.
[10] J. K. Grabski and A. Karageorghis, *Moving pseudo-boundary method of fundamental solutions for nonlinear potential problems*, Eng. Anal. Bound. Elem. **105** (2019), 78–86.
[11] H. Haddar and R. Kress, *Conformal mappings and inverse boundary value problems*, Inverse Problems **21** (2005), 935–953.
[12] U. Heise, *Numerical properties of integral equations in which the given boundary values and the sought solutions are defined on different curves*, Comput. Struct. **8** (1978), 199–205.
[13] O. Ivanyshyn and R. Kress, *Nonlinear integral equations for solving inverse boundary value problems for inclusions and cracks*, J. Integral Equations Appl. **18** (2006), no. 1, 13–38.
[14] A. Karageorghis and D. Lesnic, *Detection of cavities using the method of fundamental solutions*, Inverse Probl. Sci. Eng. **17** (2009), 803–820.
[15] A. Karageorghis and D. Lesnic, *The method of fundamental solutions for the inverse conductivity problem*, Inverse Probl. Sci. Eng. **18** (2010), 567–583.

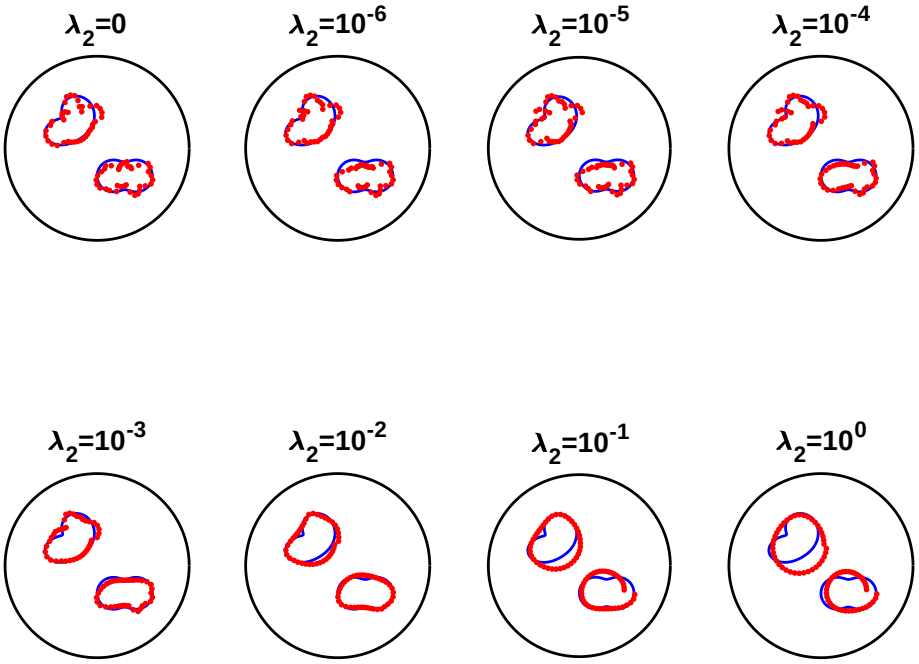

FIGURE 18. Example 5: Results for noise $p = 5\%$ and regularization with λ_2.

[16] A. Karageorghis, D. Lesnic and L. Marin, *A moving pseudo–boundary method of fundamental solutions for void detection*, Numer. Methods Partial Differential Equations **29** (2013), 935–960.
[17] A. Karageorghis, D. Lesnic and L. Marin, *A moving pseudo-boundary MFS for three-dimensional void detection*, Adv. Appl. Math. Mech. **5** (2013), 510–527.
[18] A. Karageorghis, D. Lesnic, and L. Marin, *A survey of applications of the MFS to inverse problems*, Inverse Probl. Sci. Eng. **19** (2011), 309–336.
[19] A. Karageorghis, D. Lesnic and L. Marin, *The MFS for inverse geometric problems*, in L. Marin, L. Munteanu and V. Chiroiu, Editors, *Inverse Problems and Computational Mechanics, Vol. 1*, Editura Academiei, Bucharest, Romania, 2011, pp 191-216.
[20] M. Li, C. S. Chen and A. Karageorghis, *The MFS for the solution of harmonic boundary value problems with non-harmonic boundary conditions*, Comput. Math. Applic. **66** (2013), 2400–2424.
[21] L. Marin and D. Lesnic, *The method of fundamental solutions for nonlinear functionally graded materials*, Int. J. Solids Structures **44** (2007), 6878–6890.
[22] The MathWorks, Inc., 3 Apple Hill Dr., Natick, MA, *Matlab*.
[23] L. Qiu, W. Chen, F. Wang, C.-S. Liu and Q. Hua, *Boundary function method for boundary identification in two-dimensional steady-state nonlinear heat conduction problems*, Eng. Anal. Bound. Elem. **103** (2019), 101–108.

[24] L. Rondi, *Uniqueness and Optimal Stability for the Determination of Multiple Defects by Electrostatic Measurements*, Ph.D. thesis, University of Trieste, 1999, `http://www.sissa.it/library/Thesis/rondi99.ps`.
[25] Y.-S. Smyrlis and A. Karageorghis, *Numerical analysis of the MFS for certain harmonic problems*, ESAIM: Math. Model. Numer. Anal. **38** (2004), 495–517.
[26] O. Steinbach, *Numerical Approximation Methods for Elliptic Boundary Value Problems*. Springer-Verlag, New York, 2008.
[27] F. Wang, Q. Hua and C-S. Liu, *Boundary function method for inverse geometry problem in two-dimensional anisotropic heat conduction equation*, Appl. Math. Lett. **84** (2018), 130–136.

Appendix

The outward normal vector $\boldsymbol{n}$ is defined as follows:

$$\boldsymbol{n} = \begin{cases} \cos\vartheta\,\mathbf{i} + \sin\vartheta\,\mathbf{j}\,, & \text{if} \quad \boldsymbol{x} \in \partial\Omega_2, \\ \dfrac{1}{\sqrt{r^2(\vartheta) + r'^2(\vartheta)}}\left[-\left(r'(\vartheta)\sin\vartheta + r(\vartheta)\cos\vartheta\right)\mathbf{i} + \left(r'(\vartheta)\cos\vartheta - r(\vartheta)\sin\vartheta\right)\mathbf{j}\right], & \text{if} \quad \boldsymbol{x} \in \partial\Omega_1, \end{cases}$$

where $\mathbf{i} = (1,0)$ and $\mathbf{j} = (0,1)$. As a result, from (3.1) the normal derivative $\partial_n u_N$ is evaluated as

$$\partial_n u_N = \boldsymbol{n} \cdot \nabla u_N = -\frac{1}{2\pi}\sum_{k=1}^{2N} c_k \frac{(\boldsymbol{x} - \boldsymbol{\xi}_k)\cdot \boldsymbol{n}}{|\boldsymbol{x} - \boldsymbol{\xi}_k|^2}. \tag{A.1}$$

In the above expression, we use the finite-difference approximation

$$r'(\vartheta_j) \approx \frac{r_{i+1} - r_{i-1}}{4\pi/N} = r'_j, \quad j = \overline{1,N}, \tag{A.2}$$

with the convention that $r_{N+1} = r_1$, $r_0 = r_N$, and

$$n_{x_j} = \frac{-\left(r'(\vartheta_j)\sin\vartheta_j + r(\vartheta_j)\cos\vartheta_j\right)}{\sqrt{r^2(\vartheta_j) + r'^2(\vartheta_j)}} \approx \frac{-\left(r'_j S_j + r_j C_j\right)}{\sqrt{r_j^2 + r'^2_j}} = \frac{-\left(\dfrac{r_{j+1} - r_{j-1}}{\sigma}\right) S_j - r_j C_j}{\sqrt{r_j^2 + \left(\dfrac{r_{j+1} - r_{j-1}}{\sigma}\right)^2}},$$

$$n_{y_j} = \frac{r'(\vartheta_j)\cos\vartheta_j - r(\vartheta_j)\sin\vartheta_j}{\sqrt{r^2(\vartheta_j) + r'^2(\vartheta_j)}} \approx \frac{r'_j C_j - r_j S_j}{\sqrt{r_j^2 + r'^2_j}} = \frac{\left(\dfrac{r_{j+1} - r_{j-1}}{\sigma}\right) C_j - r_j S_j}{\sqrt{r_j^2 + \left(\dfrac{r_{j+1} - r_{j-1}}{\sigma}\right)^2}}$$

where $j = \overline{1,N}$ and $\sigma = 4\pi/N$. Therefore,

$$n_{x_1} = \frac{-\left(\dfrac{r_2 - r_N}{\sigma}\right) S_1 - r_1 C_1}{\sqrt{r_1^2 + \left(\dfrac{r_2 - r_N}{\sigma}\right)^2}}$$

$$n_{x_j} = \frac{-\left(\dfrac{r_{j+1} - r_{j-1}}{\sigma}\right) S_j - r_j C_j}{\sqrt{r_j^2 + \left(\dfrac{r_{j+1} - r_{j-1}}{\sigma}\right)^2}}, \quad j = \overline{2,N-1},$$

$$n_{x_N} = \frac{-\left(\frac{r_1 - r_{N-1}}{\sigma}\right) S_N - r_N C_N}{\sqrt{r_N^2 + \left(\frac{r_1 - r_{N-1}}{\sigma}\right)^2}},$$

$$n_{y_1} = \frac{\left(\frac{r_2 - r_N}{\sigma}\right) C_1 - r_1 S_1}{\sqrt{r_1^2 + \left(\frac{r_2 - r_N}{\sigma}\right)^2}},$$

$$n_{y_j} = \frac{\left(\frac{r_{j+1} - r_{j-1}}{\sigma}\right) C_j - r_j S_j}{\sqrt{r_j^2 + \left(\frac{r_{j+1} - r_{j-1}}{\sigma}\right)^2}}, \quad j = \overline{2, N-1},$$

$$n_{y_N} = \frac{\left(\frac{r_1 - r_{N-1}}{\sigma}\right) C_N - r_N S_N}{\sqrt{r_N^2 + \left(\frac{r_1 - r_{N-1}}{\sigma}\right)^2}},$$

In the derivation of the Jacobian we shall need the following derivatives:

$$\frac{\partial n_{x_j}}{\partial r_j} = \frac{-C_j}{\sqrt{r_j^2+\left(\dfrac{r_{j+1}-r_{j-1}}{\sigma}\right)^2}} - \frac{\left(-\left(\dfrac{r_{j+1}-r_{j-1}}{\sigma}\right)S_j - r_jC_j\right)r_j}{\left(r_j^2+\left(\dfrac{r_{j+1}-r_{j-1}}{\sigma}\right)^2\right)^{3/2}}, \quad j=\overline{1,N},$$

$$\frac{\partial n_{x_j}}{\partial r_{j+1}} = \frac{-\dfrac{S_j}{\sigma}}{\sqrt{r_j^2+\left(\dfrac{r_{j+1}-r_{j-1}}{\sigma}\right)^2}} - \frac{\left(-\left(\dfrac{r_{j+1}-r_{j-1}}{\sigma}\right)S_j - r_jC_j\right)\left(\dfrac{r_{j+1}-r_{j-1}}{\sigma^2}\right)}{\left(r_j^2+\left(\dfrac{r_{j+1}-r_{j-1}}{\sigma}\right)^2\right)^{3/2}}, \quad j=\overline{1,N-1},$$

$$\frac{\partial n_{x_N}}{\partial r_1} = \frac{-\dfrac{S_N}{\sigma}}{\sqrt{r_N^2+\left(\dfrac{r_1-r_{N-1}}{\sigma}\right)^2}} - \frac{\left(-\left(\dfrac{r_1-r_{N-1}}{\sigma}\right)S_N - r_NC_N\right)\left(\dfrac{r_1-r_{N-1}}{\sigma^2}\right)}{\left(r_N^2+\left(\dfrac{r_1-r_{N-1}}{\sigma}\right)^2\right)^{3/2}},$$

$$\frac{\partial n_{x_j}}{\partial r_{j-1}} = \frac{\dfrac{S_j}{\sigma}}{\sqrt{r_j^2+\left(\dfrac{r_{j+1}-r_{j-1}}{\sigma}\right)^2}} - \frac{\left(\left(\dfrac{r_{j+1}-r_{j-1}}{\sigma}\right)S_j + r_jC_j\right)\left(\dfrac{r_{j+1}-r_{j-1}}{\sigma^2}\right)}{\left(r_j^2+\left(\dfrac{r_{j+1}-r_{j-1}}{\sigma}\right)^2\right)^{3/2}}, \quad j=\overline{2,N},$$

$$\frac{\partial n_{x_1}}{\partial r_N} = \frac{\dfrac{S_1}{\sigma}}{\sqrt{r_1^2+\left(\dfrac{r_2-r_N}{\sigma}\right)^2}} - \frac{\left(\left(\dfrac{r_2-r_N}{\sigma}\right)S_1 + r_1C_1\right)\left(\dfrac{r_2-r_N}{\sigma^2}\right)}{\left(r_1^2+\left(\dfrac{r_2-r_N}{\sigma}\right)^2\right)^{3/2}},$$

and

$$\frac{\partial n_{y_j}}{\partial r_j}=\frac{-S_j}{\sqrt{r_j^2+\left(\frac{r_{j+1}-r_{j-1}}{\sigma}\right)^2}}-\frac{\left(\left(\frac{r_{j+1}-r_{j-1}}{\sigma}\right)C_j-r_jS_j\right)r_j}{\left(r_j^2+\left(\frac{r_{j+1}-r_{j-1}}{\sigma}\right)^2\right)^{3/2}},\ j=\overline{1,N},$$

$$\frac{\partial n_{y_j}}{\partial r_{j+1}}=\frac{\frac{C_j}{\sigma}}{\sqrt{r_j^2+\left(\frac{r_{j+1}-r_{j-1}}{\sigma}\right)^2}}-\frac{\left(\left(\frac{r_{j+1}-r_{j-1}}{\sigma}\right)C_j-r_jS_j\right)\left(\frac{r_{j+1}-r_{j-1}}{\sigma^2}\right)}{\left(r_j^2+\left(\frac{r_{j+1}-r_{j-1}}{\sigma}\right)^2\right)^{3/2}},\ j=\overline{1,N-1},$$

$$\frac{\partial n_{y_N}}{\partial r_1}=\frac{\frac{C_N}{\sigma}}{\sqrt{r_N^2+\left(\frac{r_1-r_{N-1}}{\sigma}\right)^2}}-\frac{\left(\left(\frac{r_1-r_{N-1}}{\sigma}\right)C_N-r_NS_N\right)\left(\frac{r_1-r_{N-1}}{\sigma^2}\right)}{\left(r_N^2+\left(\frac{r_1-r_{N-1}}{\sigma}\right)^2\right)^{3/2}},$$

$$\frac{\partial n_{y_j}}{\partial r_{j-1}}=\frac{-\frac{C_j}{\sigma}}{\sqrt{r_j^2+\left(\frac{r_{j+1}-r_{j-1}}{\sigma}\right)^2}}+\frac{\left(\left(\frac{r_{j+1}-r_{j-1}}{\sigma}\right)C_j-r_jS_j\right)\left(\frac{r_{j+1}-r_{j-1}}{\sigma^2}\right)}{\left(r_j^2+\left(\frac{r_{j+1}-r_{j-1}}{\sigma}\right)^2\right)^{3/2}},\quad j=\overline{2,N},$$

$$\frac{\partial n_{y_1}}{\partial r_N}=\frac{-\frac{C_1}{\sigma}}{\sqrt{r_1^2+\left(\frac{r_2-r_N}{\sigma}\right)^2}}+\frac{\left(\left(\frac{r_2-r_N}{\sigma}\right)C_1-r_1S_1\right)\left(\frac{r_2-r_N}{\sigma^2}\right)}{\left(r_1^2+\left(\frac{r_2-r_N}{\sigma}\right)^2\right)^{3/2}}.$$

Department of Mathematics and Statistics, University of Cyprus/ Πανεπιστημιο Κυπρου, P.O.Box 20537, 1678 Nicosia/Λευκωσια, Cyprus/Κυπρος
E-mail address: andreask@ucy.ac.cy

Department of Applied Mathematics, University of Leeds, Leeds LS2 9JT, UK
E-mail address: amt5ld@maths.leeds.ac.uk

Department of Mathematics, Faculty of Mathematics and Computer Science, University of Bucharest, 14 Academiei, 010014 Bucharest, and Gheorghe Mihoc – Caius Iacob Institute of Mathematical Statistics and Applied Mathematics of the Romanian Academy, 13 Calea 13 Septembrie, 050711 Bucharest, Romania
E-mail address: liviu.marin@fmi.unibuc.ro; marin.liviu@gmail.com